

Generalizability of Neuromuscular Coordination in the Human Upper Extremity after Stroke and its Implications in Neurorehabilitation

Manuel Portilla-Jiménez

University of Houston

Yoon No Gregory Hong

University of Houston

Komal K. Kukkar

University of Houston

Hyung-Soon Park

Korea Advanced Institute of Science and Technology

Sheng Li

University of Texas Health Science Center - Houston

Jinsook Roh

jroh@uh.edu

University of Houston

Research Article

Keywords: Stroke, motor control, muscle synergy, neurorehabilitation, electromyography, isometric force generation, dynamic reaching

Posted Date: July 18th, 2025

DOI: https://doi.org/10.21203/rs.3.rs-7078115/v1

License: @ (1) This work is licensed under a Creative Commons Attribution 4.0 International License. Read Full License

Additional Declarations: No competing interests reported.

Abstract

Background

Previous studies have shown that stroke often impairs neuromuscular coordination (i.e., muscle synergies) across various biomechanical conditions. In our previous study, we investigated the generalizability of muscle synergies between isometric and free dynamic reaching in healthy individuals. However, the extent to which muscle synergy characteristics after stroke are generalized across these conditions remains unclear.

Methods

Electromyographic (EMG) signals from eight upper extremity muscles were recorded from 14 chronic stroke survivors with mild-to-severe motor impairment and eight age-range matched controls while performing isometric force generation and point-to-point dynamic reaching tasks. Non-negative matrix factorization was applied to identify muscle synergy characteristics underlying each task.

Results

In both groups, muscle activation patterns were effectively reconstructed using a small set of muscle synergies. The neurologically intact participants recruited four and five muscle synergies during the static and dynamic tasks, respectively. However, stroke survivors typically recruited four muscle synergies to perform both tasks. In addition, the composition of muscle synergies within each participant in both groups was largely conserved across the two tasks, though alterations in intermuscular coordination patterns were observed in post-stroke individuals, particularly in moderate and severe impairment cases. The majority of the altered, stroke-induced synergy patterns were explained by merging synergies underlying dynamic reaching of healthy individuals. The characteristics of muscle synergy activation profiles differed between the isometric and dynamic motor tasks in both groups. Stroke-induced alterations in correlation of pairs of synergy activation profiles were observed in dynamic reaching, but not in isometric conditions.

Conclusion

This study provides several implications to stroke neurorehabilitation. First, accessible isometric conditions, especially for severely impaired stroke survivors, can be adopted as biomechanical conditions of therapeutic exercises expecting potential transferability of motor learning effects to dynamic conditions. Second, fractionation of merged synergies after stroke can be a potential rehabilitation target to enhance motor control. Finally, dynamic tasks can be effective in assessing and intervening in potential motor abnormalities that may not be prominent during isometric conditions. These results highlight the importance of developing novel stroke rehabilitation strategies that aim at improving intermuscular coordination characteristics to enhance motor function across varying biomechanical conditions after stroke.

BACKGROUND

Stroke is a leading cause of permanent disability globally. It often results in upper extremity (UE) motor impairment and negatively affects the ability to perform a variety of essential activities of daily living ranging from static (i.e., isometric force generation) to dynamic motor tasks. Neuromuscular coordination strategies vary under different biomechanical conditions in neurologically intact individuals and stroke survivors. These strategies require the coordination of the complex musculoskeletal system with the control performed by the central nervous system (CNS). Fundamental neurophysiological questions, particularly after stroke, include how the CNS selects an appropriate muscle activation pattern from many possible options, and how this selection process is altered following brain injury (1, 2). A simplified

model, which is based on more than two decades of animal and human studies, suggests that instead of managing every muscle individually, the CNS orchestrates movements by decreasing the large number of degrees of freedom to a limited set of motor modules or muscle synergies (3–6). Here, muscle synergies are defined as a consistent ratio of muscle coactivation across multiple muscles necessary to perform voluntary movements. It is important to distinguish the term "motor modules or muscle synergies" from the abnormal stroke synergies (i.e., the clinical flexor synergy and the clinical extensor synergy), which are stereotypical joint couplings (7, 8). In addition, many studies have described altered intermuscular coordination in the arm as stroke-induced abnormalities under different biomechanical conditions (e.g., isometric force control, dynamic reaching, or grasping) (9–11). Moreover, recent studies have targeted muscle synergy characteristics to develop novel rehabilitation strategies to improve motor control after stroke underlying isometric force generation (12–14) and dynamic conditions (15, 16). Therefore, the muscle synergy concept can be an effective strategy not only for evaluating but also for improving abnormal intermuscular muscular coordination after stroke underlying varying movements (17, 18).

Muscle synergies identified during isometric force generation or dynamic conditions provide a valuable approach for investigating abnormal neuromuscular coordination in stroke survivors. First, studies underlying static conditions have shown abnormal muscle synergy patterns after stroke compared with healthy individuals (9, 19). For instance, Roh et al. found that severely impaired stroke survivors often abnormally co-activated the anterior deltoid fibers with medial and posterior deltoid fibers in the composition of the shoulder abductor/extensor synergy (9), whereas in healthy individuals, anterior deltoid fibers were co-activated with the pectoralis major within the shoulder adductor/flexor synergy pattern. In addition, the pectoralis clavicular major was activated with an atypical reduction of the activation of the anterior and medial deltoid during isometric shoulder adduction and flexor tasks. A further study demonstrated that these strokeinduced alterations were observed even in mildly and moderately impaired stroke survivors, and that as motor impairment increased, the likelihood of exhibiting these abnormalities in muscle synergy composition also increased (19). Second, previous studies underlying dynamic conditions also showed abnormal stroke-induced muscle synergy characteristics (2, 10, 20-22). For example, an intermuscular coordination study during isokinetic movements, involving the shoulder and elbow joints, found that stroke survivors exhibited altered synergy activation coefficients, which were negatively correlated with the severity of motor impairments (22). Another study that required coordination between the shoulder and elbow showed that stroke-induced alterations in muscle synergies were more variable and less consistent compared to healthy individuals during hand-to-mouth and reaching movements (2). This study also found that merging was the most prominent abnormal pattern, especially in those with moderate motor impairment, resulting in a reduced independence of muscle activation modules. These findings underscore the impact of stroke on static and dynamic motor control and the potential of muscle synergy analysis to quantify these abnormalities. However, the extent to which these abnormalities are generalized across different biomechanical conditions after stroke is still unclear.

Novel neuromuscular rehabilitation exercises in various biomechanical conditions have been developed to alter atypical neuromuscular coordination after stroke to potentially improve motor control. For instance, our previous pilot studies underlying isometric exercises through human-machine interaction have shown the potential to modulate neuromuscular coordination patterns in the UE after stroke, even in severely impaired stroke patients, to reduce motor impairment measured by the Fugl-Meyer Assessment (FMA) (12–14). A longitudinal study demonstrated the feasibility of inducing new intermuscular coordination, and expanding the repertoire of muscle synergies in chronic stroke survivors (13). A further neuromuscular-coordination-guided study in static condition showed that stroke-induced neuromuscular coordination can be malleable to become similar to patterns observed in healthy populations (12). In addition, functional electrical stimulation (FES) training underlying dynamic conditions provided evidence that stroke participants could improve muscle synergy composition and motor performance by using muscle synergy characteristics identified from neurologically intact volunteers (15, 16). Indeed, Niu et al. showed that after only five FES reaching training sessions, stroke survivors were able to modulate not only muscle synergy compositions but also their respective activation profiles in the more affected arm. Overall, these studies suggest that stroke-induced intermuscular coordination is malleable and can be

enhanced by targeting muscle synergy characteristics in a rehabilitation exercise; nevertheless, the appropriate selection of biomechanical conditions to optimally improve neuromuscular coordination characteristics remains unsettled.

Considering these previous studies that showed stroke survivors utilized a small number of motor modules to perform both static and dynamic motor tasks, a key question arises: to what extent are post-stroke muscle synergy characteristics shared across different biomechanical conditions in the arm? In our previous study, we investigated the generalizability of intermuscular coordination between isometric force generation and free point-to-point reaching across different starting arm positions in young, neurologically intact adults (23). This study found evidence of muscle synergy patterns shared between the two tasks. In addition, synergy activation profiles were mainly preserved within the same task across different arm positions, but they differed between static and dynamic tasks. Similarly, a lower extremity (LE) study showed evidence of shared muscle synergies between cycling and walking after stroke, and a reduction in the number of muscle synergies compared with healthy individuals, especially for severely and moderately impaired survivors (24). Although these findings suggest both shared and task-specific characteristics of muscle synergies in young individuals in the UE and stroke survivors in the LE, it remains unclear whether stroke-induced UE intermuscular coordination composition exhibits similar levels of generalization across different motor behaviors. Understanding which muscle synergy characteristics are shared across different biomechanical conditions and which are task-dependent is relevant for neurorehabilitation because it could guide the design and targeting of novel intervention strategies. Additionally, evidence of similar muscle synergy patterns in the UE across varying biomechanical conditions after stroke could provide evidence of potential transferability of neuromuscular coordination improvements from a training task (e.g., isometric training) to an untrained task (e.g., dynamic movements).

Thus, the objective of this study was to investigate the generalizability of intermuscular coordination after stroke between isometric force generation and free dynamic tasks. We hypothesized that, despite the level of motor impairment, stroke survivors will exhibit shared intermuscular coordination patterns between these two biomechanical conditions. Fourteen stroke survivors and eight age-range-matched healthy controls were recruited and performed the two tasks in two planes (horizontal and frontal) while the surface electromyographic (EMG) signals from the eight main UE muscles were recorded. The same robotic device was used for both tasks and NNMF was applied to identify muscle synergy patterns and their respective activation profiles.

METHODS

Participants

Fourteen stroke survivors [8 males, 57.5 ± 8.79 years (mean \pm standard deviation (SD)] and eight age-range-matched neurologically intact volunteers [5 males, 50.75 ± 8.05 years] participated in this study. Stroke participants were grouped into one of the three subgroups based on their level of motor impairment measured by the Upper Extremity Fugl-Meyer Assessment (UE-FMA) (max score = 66 points) as follows: 1) mildly impaired (number of participants (n) = 4, UE-FMA ≥ 50); 2) moderately impaired (n = 5, $26 \le UE$ -FMA ≤ 50); and 3) severely impaired (n = 5, UE-FMA ≤ 26) (Table 1). The clinical assessments (FMA) were performed by licensed physical therapists. The inclusion criteria for stroke participants were as follows: 1) single unilateral ischemic or hemorrhagic stroke, 2) chronic hemiparesis (at least 6 months after stroke onset), 3) age range: 40 to 75, 4) not receiving botulinum toxin on the more affected arm within 3 months, 5) absence of cognitive impairment that would prevent understanding the experimental task and provide written informed consent (mini-mental status examination (MMSE) score of 24 or higher), and 6) no presence of any other neurological pathology or orthopedic disorder in the UE. The healthy individuals had no muscular or orthopedic impairment in the UE. This study followed the guidelines of the Declaration of Helsinki, with the approval of the University of Houston Institutional Review Board. All participants provided informed written consent before the beginning of the study.

Equipment

The KAIST Upper Limb Synergy Investigation System (KULSIS) (25) was used for both biomechanical conditions (isometric force generation and free dynamic reaching; Fig. 1A). The three-dimensional force/torque device is measured at hand by a six-degree-of-freedom load cell (Model: 45E15A4, JR3, Woodland, CA). Eight major UE muscles were recorded by the surface EMG system (Trigno Wireless Biofeedback System; Delsys Inc., MA, USA). The muscles recorded included brachioradialis (BRD), biceps brachii (BB), triceps brachii (long and lateral heads) (TrLo and TrLa, respectively), deltoids (anterior, middle, and posterior fibers; AD, MD, and PD, respectively), and pectoralis major clavicular head (PEC). EMG data and 3D force data were synchronized and recorded using a custom-design code written in LabVIEW software (National Instruments, TX, USA). The EMG and force signals were collected at a sampling rate of 1 kHz.

Experimental Design

The study consisted of two distinct biomechanical conditions: isometric force generation and free dynamic reaching (no resistance; minimal friction). Both tasks were performed using the more affected arm for stroke survivors and the dominant arm for healthy participants. Each participant's full arm length, defined as the distance from the acromion to the center of the fist was measured before starting the task. For both tasks, participants grasped the handle while seated with their hand positioned in front of the shoulder at a distance of 70% of the full arm length (Fig. 1A). To maximize the variability of the EMG and to decrease any potential bias in the target force direction, two planes (horizontal and frontal) were included each of them with 12 targets equally spaced on each plane. In addition, the participants wore a seatbelt to constrain trunk posture and upper body movement. To maintain consistency in the grasping posture, the participants wore an auxiliary training glove. At the beginning of each task, the KULSIS's handle supported the participant's relaxed arm against gravity. Then, the load cell connected to the handle was zeroed to eliminate any force signal associated with the weight of the arm for an accurate measurement of the 3D forces.

For the isometric force generation task, the maximum lateral force (MLF) that each participant could generate with the hand positioned in the starting arm location was estimated at the beginning of the task. A force level corresponding to 40% of the MLF was used to determine the force load for the target-matching task in both planes. Our previous study showed that the MLF is typically the weakest maximum voluntary contraction among the six cardinal directions (9). As a result, defining the target force magnitude by using a percentage of the MLF facilitated matching the force target in any direction within the two tested planes. The task involved matching twenty-four force targets, with three repetitions per target location. Twelve targets were evenly spaced around a circumference in the horizontal plane, and the other twelve were distributed similarly in the frontal plane (Fig. 1B). The targets were randomized within each plane, and the order of the two planes was randomized across participants. Each trial consisted of three seconds for inter-trial interval, two seconds of baseline for further EMG processing, and up to ten seconds to match the targets successfully. For a successful trial, participants had to maintain the cursor in the desired force direction within a 20% logical radius of the targeted force for one second. If an attempt was missed, another attempt was allowed in the same direction, with a maximum of three attempts per target repetition.

For the free dynamic reaching task, participants performed a center-out task directed towards one of the twenty-four targets, which were equally distributed on two planes (horizontal and frontal). The KULSIS's end effector is constrained to move linearly along the rail. Similar to the isometric conditions, twelve targets were positioned in the horizontal plane, whereas the remaining twelve were arranged in the frontal plane. The KULSIS's rail was randomly positioned into one of the six locations (Fig. 1C) for each plane. A goniometer was used to manually measure these six positions of the rail. The task involved matching twenty-four center-out reaching targets. For each rail location, two out of the twelve targets were randomly display, with three repetitions per target location. Each trial included a three-second inter-trial interval, followed by a two-second baseline period for further EMG processing, and up to four seconds to successfully match the target. For a successful trial, participants had to move the handle from the starting arm location to a position within a range of 10 to 12 cm and hold within this range for 0.5 seconds. If participants missed an attempt, they were given another chance in the same target direction, with a maximum of three attempts allowed for each target repetition.

Data Analysis

The raw EMG data were processed using customized MATLAB software. First, electrocardiogram (ECG) artifacts were visually inspected and removed with a wavelet-based filtering method. Second, to eliminate the DC offset, the mean baseline was subtracted from the processed EMG signal. Full-wave rectification was then applied, followed by another subtraction of the mean baseline to reduce baseline noise. Finally, to obtain the EMG signal envelope, full-wave rectification and a low pass filter (4th order Butterworth filter with a 10 Hz cutoff frequency) were applied.

For the isometric task, the EMG data for each trial were trimmed to include only the muscle activation during the one-second holding period. On the other hand, to trim the point-to-point reaching EMG data, the onset and offset were identified at the points where the handle's movement speed exceeded or dropped below 10% of the maximum velocity, respectively (Fig. 2). For both tasks, only matched trials were included, and each trial was interpolated to 100 samples to ensure that all trials contributed equally to the identification of muscle synergies. Finally, the EMG data were concatenated across the 24 trials for each biomechanical condition, and each muscle was normalized by its own variance to prevent bias from muscles with high variance during muscle synergy identification.

Muscle Synergy Identification

Non-negative matrix factorization (NNMF) was applied to the pre-processed EMG data for each task to extract muscle synergies. To satisfy the non-negativity requirement of NNMF, any negative pre-processed EMG value was replaced with zero. The EMGs from the eight-arm muscle were represented as a linear combination of a set of the time-invariant muscle synergy vectors (W) and their corresponding activation profiles (C) as follows:

$$EMG_{MATRIX} \approx W \bullet C$$

where W is an M (number of muscles = 8) by N (number of muscle synergies) matrix, and where C is an N by D (number of data sample points) matrix.

To identify the minimum number of muscle synergies that adequately reconstructed the spatial characteristics of the EMGs, the variance accounted for (VAF) was calculated using the entire dataset, referred to as global VAF (gVAF). The VAF was defined by the next formula:

$$VAF = 100 \left(1 - \frac{SSE}{SST} \right)$$

where SSE is the sum of the squared residuals and STT is the summation of the squared EMG data (19). The criteria for identifying the optimal number of muscle synergies included 90% gVAF or higher and at least a 5% difference of gVAF (diffVAF) when an additional synergy was included (26).

Calculating Muscle Synergy Similarities

The similarity of muscle synergy composition between isometric force generation and dynamic reaching tasks was evaluated by calculating the scalar product of the best-matched pairs of muscle synergy vectors across all possible combinations within each participant (27). To determine the similarity threshold, 1000 random sets of muscle synergy patterns were generated by randomly selecting muscle weights from those computed synergies underlying all participants and both tasks. Each random synergy vector was then normalized by dividing by its magnitude to obtain unit vectors. Scalar products were calculated for all possible pairs of these muscle synergies, which were sorted in ascending order, and the statistical threshold was set at the 95th percentile of these values (19). Thus, the similarity index threshold was estimated to be 0.819. Therefore, if the scalar product of a pair synergy is greater than this threshold, these synergies will be considered statistically significant (p<0.05), indicating similar muscle synergy patterns.

Merging Synergy Analysis

To assess the merging of muscle synergies identified from healthy individuals in to explain abnormalities in stroke-induced synergies, norm (model) synergies from the healthy group were created by organizing all healthy participant synergies based on the best-matched pairs of muscle synergy vectors across all possible combinations. Muscle weights were then averaged across participants within the same motor task, and the resulting synergy vectors were normalized by their respective magnitudes to obtain the norm synergies. Next, each synergy from stroke survivors was directly compared with each of the norm synergies of healthy participants. If the highest dot product between a stroke-induced synergy and any norm synergy exceeded the similarity threshold (0.819), that synergy was considered preserved because it is statistically similar to a norm synergy. However, if the highest dot product was below the threshold, the synergy was classified as altered, indicating that no norm synergy from the healthy group could explain it.

Each altered, stroke-induced synergy was reconstructed as a non-negative linear combination of healthy model synergies. The non-negative least square method was implemented to find the coefficients (MATLAB's Isqnonneg function), with a threshold of 0.3 (28). To apply this method, each altered, stroke-induced synergy was then reconstructed as a linear combination of two norm synergies from the healthy group. The dot product between the normalized reconstructed synergy and the original abnormal synergy was computed. If this value exceeded the similarity threshold (0.819), the altered synergy was considered to be explainable by merging two norm synergies.

Number of Synergies Required per Target Direction

To identify the number of muscle synergies activated for each of the twenty-four target directions, only those synergy activation profile values that surpassed a defined threshold were considered. To define this threshold, activation profile values were combined across all muscle synergies, trials, and participants (healthy control and stroke participants were divided into two groups for this analysis) within the same task. Then, a change point detection method was used to detect a sudden change in the variance of the data (findchangepts function MATLAB) (23).

Additional Statistical Tests

The number of muscle synergies significantly activated across the 24 target directions per task within each of the four subgroups did not follow a normal distribution, as determined by the Shapiro-Wilk test. Therefore, the non-parametric Wilcoxon signed-rank test was used to test statistically differences between tasks within each subgroup. *P*-values lower than 0.05 were considered significant.

Spearman's rank correlation analysis was performed to evaluate the monotonic relationship between all possible pairs of averaged synergy activation profiles underlying each motor task within each subgroup. Correlations were considered statistically significant at p < 0.05.

RESULTS

EMG Patterns of Two-Dimensional Isometric Force Generation and Dynamic Reaching

The EMG signals recorded in neurologically intact volunteers and stroke survivors showed distinct muscle activity underlying isometric force generation and dynamic reaching. For instance, Fig. 2 shows the EMG patterns from two representative participants (a healthy volunteer and a moderately impaired stroke survivor) performed during static and dynamic tasks in a medial direction target in the horizontal plane. The healthy volunteer mainly recruited AD, MD, and PEC during the isometric force generation trial (Fig. 2A), while BRD, BB, AD, and PEC were activated during the dynamic reaching (Fig. 2B). In contrast, the stroke participant mainly recruited BB and PEC during the static trial, while mainly PEC, with some activation of AD and BB, was recruited for the dynamic trial. Over time, the EMG signal magnitudes varied between the two tasks for both participants.

Optimal Number of Muscle Synergies in Isometric Force Generation and Dynamic Reaching Tasks

The number of muscle synergies required to explain EMG variance differed between tasks in healthy individuals but remained consistent in stroke survivors. Figure 3 shows the average number of muscle synergies for both groups across the two tasks. Based on the criteria described in the previous section (see **Method section**, Muscle Synergy Identification), on average, four synergies $(3.75 \pm 0.89; \text{mean} \pm \text{SD})$ were required to account for the variance of the EMG underling the isometric force generation in the healthy individuals (n = 8), while five synergies (4.75 ± 0.83) were required for the dynamic reaching task in the same group. Similarly, for the stroke survivors (n = 14), four synergies were typically required for both tasks, isometric force generation (3.93 ± 0.83) and dynamic reaching (4.29 ± 0.47) . A significant difference was found in the optimal number of muscle synergies in the healthy group between tasks (paired t-test, p < 0.05), but not in the stroke population.

Muscle Synergy Patterns

Muscle synergy patterns were consistent across both isometric force generation (Fig. 4A) and dynamic reaching (Fig. 4B) tasks within each subgroup, including healthy individuals, and mildly, moderately, and severely impaired stroke subgroups. The synergy patterns were named following the appropriate mechanical action of the muscles mainly activated within each synergy. The muscle synergies of the healthy participants activated during both isometric force generation and dynamic reaching tasks were as follows: elbow flexor (EF), elbow extensor (EE), shoulder flexor/adductor (SF/Ad), and shoulder extensor/abductor (SE/Ab). The fifth synergy of dynamic reaching was named shoulder adductor (SAd) because of its functional activation during the task performance. The EF synergy included the activation of elbow flexor muscles (BRD and BB). The EE synergy consisted of the activation of elbow extensor muscles (TrLo and TrLa). The SF/Ad consisted of the activation of AD, MD, and PEC. The SE/Ab synergy contained the activation of MD and PD. The SAd synergy contained the activation of PEC with some activation of BB.

Similarly, the muscle synergies from the three stroke subgroups (mildly, moderately, and severely impaired stroke survivors) included: EF, EE, SF/Ad, and SE/Ab. However, systematic alterations were observed in stroke participants, especially in moderately and severely impaired subgroups. The EF synergies mainly consisted of BRD and BB with some co-activation of TrLa, AD, and MD for the two tasks. In addition, SF/Ad synergies mainly consisted of PEC with an abnormal reduction of AD and MD, and an atypical co-activation with BB for moderately and severely impaired subgroups. These abnormal patterns were not typically observed during the two-dimensional isometric force generation and dynamic reaches in the mildly impaired stroke subgroup.

Within-Subject Similarity of Muscle Synergy Composition between Isometric Force Generation and Dynamic Reaching Tasks

The majority of the synergies were statistically similar (threshold [n] = 0.819; p < 0.05) between isometric force generation and dynamic reaching within each individual of each subgroup (Fig. 5). In healthy individuals, all four muscle synergies were significantly similar between the two tasks. For instance, in the EF and EE synergies, the similarity indices [mean \pm SD] were 0.85 \pm 0.13 and 0.88 \pm 0.10, respectively. Additionally, the similarity indices of the SF/Ad and SE/Ab synergies were 0.84 \pm 0.09 and 0.86 \pm 0.10, respectively. Similarly, in the mildly impaired stroke subgroup, all four synergies were statistically similar between the static and dynamic tasks. In both the moderately and severely impaired stroke subgroups, three out of the four identified synergies were similar, including EE, SF/Ad, and SE/Ab synergies. In contrast, the similarity index of the EF synergy was not statistically similar in either subgroup (moderate: 0.80 \pm 0.11; severe: 0.76 \pm 0.17). The elbow flexor synergy was not statistically similar between the two tasks in the moderately and severely impaired subgroups, mainly because of the greater variability in the muscle weights of elbow flexor muscles (BRD and BB) with an elbow extensor (TrLa) and a shoulder adductor (AD) within the same participant across both tasks.

Altered, Stroke-Induced Synergies Explained as Merging of Synergies of Healthy Individuals

Altered, stroke-induced muscle synergies observed during both isometric force generation and dynamic reaching were explained as a linear combination of muscle synergies underlying dynamic reaches of healthy participants. The mean of muscle synergies underlying dynamic reaching in the healthy group formed the norm (model) synergies. The scalar products of the best-matched synergy pairs between the norm synergies and each stroke participant's synergies underlying each motor task were calculated. Regarding the static task, 41 out of the 56 synergies (14 stroke survivors × 4 synergies per participant) of all the stroke participants were identified as preserved (i.e., the scalar product greater than the threshold (0.819); see Methods section, Calculating Muscle Synergy Similarities). Similarly, 42 out of the 56 synergies of the 14 stroke survivors were also identified as preserved during dynamic reaching. Moreover, by merging two norm (model) synergies observed from healthy individuals during the dynamic task, nine out of 13 altered, stroke-induced synergies in the isometric task, and 12 out of 14 altered synergies in the dynamic task were successfully reconstructed (i.e., the scalar products between the altered synergies and merged synergies were greater than the threshold). This finding indicates that merging or co-activation of synergies recruited during dynamic reaching in healthy conditions can largely account for abnormal synergy patterns observed after stroke across both static and dynamic motor tasks. In contrast, merging the model synergies underlying the isometric conditions could not reconstruct the same altered, stroke-induced synergies as much as the merging the model synergies underlying the dynamic conditions (i.e., only less than half of altered synergies were explained). This observation highlights that merging synergies underlying dynamic reaches of healthy individuals provides a better explanation of altered, stroke-induced muscle synergies than merging synergies underlying static tasks.

Finally, we assessed the impact of the merging on the similarity index and found that it consistently increased beyond the synergy similarity threshold (0.819), with values typically approaching 0.9. This increase in similarity was significant within each task, showing that merging dynamic synergies of healthy individuals closely resembled the altered muscle synergy patterns during both tasks (Fig. 6). Altered, stroke-induced synergies that were not able to be explained by merging as a linear combination of model synergies were not included in this analysis.

Differences in Muscle Synergy Recruitment during Isometric Force Generation and Dynamic Reaching

The static and dynamic tasks tended to adopt different muscle synergy recruitment strategies. These patterns were based on the averaged activation profiles within each subgroup, including healthy individuals, and mildly, moderately, and severely impaired participants. For visualization purposes, the 24 target directions were divided into two sets: one representing the 12 target directions from the horizontal plane (Fig. 7) and the other representing the 12 target directions from the frontal plane (Fig. 8). In the horizontal plane, synergy activation profiles appeared more directionally tuned during isometric force generation than during dynamic reaching across all subgroups, except for the severely impaired stroke subgroup (Fig. 7A vs. 7B). Furthermore, task-specific variations in synergy recruitment between isometric and dynamic motor control were reflected in terms of the number of synergies used per target direction. Healthy participants generally recruited one more muscle synergy per target direction in dynamic reaching than in isometric force generation in the horizontal plane; however, severely impaired stroke survivors generally recruited one more muscle synergy per target direction in isometric force generation than in dynamic reaching (Fig. 7C). No difference between the two tasks was observed in the mildly and moderately impaired subgroups in the number of recruited synergies per target in the horizontal plane. For healthy individuals, the activation thresholds of isometric force generation (t_iso) and dynamic reaching (t_kin) thresholds were t_iso_healthy = 1 and t_kin_healthy = 0.88 in the healthy group, whereas for the stroke groups, they were t_iso_stroke = 0.88 and t_kin_stroke = 0.85.

Similarly, Fig. 8 shows that the averaged activation profile of each muscle synergy was more tuned in the isometric force generation task (Fig. 8A) than in the dynamic reaching (Fig. 8B) in the frontal plane for healthy individuals, and mildly, and moderately impaired stroke participants, but not for severely impaired stroke survivors. Meanwhile, during the dynamic reaching, several muscle synergies were activated per target direction for all subgroups, except for the severely impaired subgroup, suggesting that multiple synergies need to be activated to perform the desired point-to-point dynamic reaching in the healthy group as well as in the mildly and moderately impaired stroke subgroups. In addition, differences were

observed in the number of muscle synergies significantly activated across the 12 target directions in the frontal plane. Healthy participants tended to recruit one more muscle synergy per target direction during the dynamic reaching than during with the static task. Interestingly, severely impaired stroke survivors generally recruited one more muscle synergy per target direction during isometric force generation than during dynamic reaching (Fig. 8C). Consistent with the horizontal plane, no difference in the number of recruited synergies per target in the frontal plane was observed between the two tasks in mildly and moderately impaired subgroups.

Even though variability was observed across subgroups, the averaged synergy activation profiles as a function of the target force direction across both planes were generally aligned with the expected mechanical action of the muscles predominantly activated within each respective muscle synergy pattern. For instance, in the horizontal plane (Fig. 7A) during the isometric task across subgroups, the EF and EE synergies were mostly activated in the backward-medial and forward-lateral directions, respectively, whereas the SF/Ad and SE/Ab synergies were more active in the medial and lateral directions, respectively. Similarly, in the dynamic reaching, the activation of EF, EE, and SF/Ad in the healthy subgroup retained similar directional preferences, whereas the preferred activation of SE/Ab shifted toward a backward-lateral direction in the horizontal plane (Fig. 7B).

The number of average muscle synergies significantly activated per target direction, with both planes combined, varied between isometric force generation and dynamic tasks in healthy individuals and severely impaired stroke survivors. Figure 9 shows the number of synergies activated and averaged across the 24 targets (12 horizontal and 12 frontal) for the four subgroups. The Wilcoxon signed-rank test between corresponding subgroups across the two tasks showed a significant difference in the number of synergies activated across the 24 target directions in the healthy individuals (p < 0.05), suggesting that the reaching task was more complex. Interestingly, for the severe subgroup, a significant difference was also found, with the isometric task typically requiring one more synergy significantly activated per target direction than the dynamic task (p < 0.01), suggesting abnormal muscle synergy recruitment strategies in the neuromuscular coordination of motor tasks in stroke survivors with severe motor impairment.

Correlation of a Pair of Synergy Activation Profiles

The trend in the correlation of any possible pairs of averaged synergy activation profiles was different between isometric force generation (Fig. 10A) and dynamic reaching (Fig. 10B) (Spearman's rank correlation, p < 0.05). During the isometric task, the elbow flexor and extensor synergy activations were negatively correlated in healthy individuals (rho = -0.84, p < 0.001) as well as in all three-stroke subgroups (rho = -0.9, p < 0.001, mild; rho = -0.73, p < 0.001, moderate; and rho = -0.77, p < 0.001, severe). Additionally, the preservation of a negative correlation even after stroke was observed between the shoulder antagonistic synergies (SF/Ad and SE/Ab) for the healthy individuals (rho = -0.48, p < 0.02) and the three-stroke subgroups (rho = -0.57, p < 0.01, mild; rho = -0.74, p < 0.01, moderate; and rho = -0.72, p < 0.001, severe). Additionally, positive correlations between agonistic synergies across both arm joints (EF and SF/Ad) were consistently maintained for three subgroups (rho = 0.55, p < 0.01, healthy; rho = 0.68, p < 0.001, mild; rho = 0.58, p < 0.01, moderate), but not for the severe subgroup (rho = 0.3, p = 0.15). Finally, the negative correlations between antagonistic synergies across both arm joints (EE and SF/Ad) were found to be kept in the four subgroups (rho = -0.77, p < 0.001, healthy; rho = -0.78, p < 0.001, mild; rho = -0.58, p < 0.01, moderate; and rho = -0.44, p < 0.05, severe). These results suggest that the correlation between any possible pairs of the averaged synergy activation profiles within each subgroup remains preserved mainly in the isometric condition, even after stroke.

In contrast, in the dynamic condition, a significant negative correlation between elbow flexor and extensor synergy activations was not observed in the healthy individuals (rho = -0.05, p = 0.82) or the mildly impaired stroke subgroup (rho = -0.39, p = 0.06), but in the moderately impaired (rho = -0.54, p < 0.01) and severely impaired (rho = -0.46, p < 0.05) impaired stroke subgroups. Similarly, the shoulder antagonistic synergies (SF/Ad and SE/Ab) did not exhibit a significant negative correlation for healthy (rho = 0.11, p = 0.59) and mildly impaired stroke survivors (rho = -0.14, p = 0.5), but they did for moderately impaired (rho = -0.58, p < 0.01) and severely impaired subgroups (rho = -0.5, p < 0.05). Interestingly, in

participants with severe motor impairment, positive coupling was identified between the elbow flexor and shoulder extensor/abductor synergies (rho = 0.75, p < 0.001).

DISCUSSION

The current study aimed at investigating the effects of different biomechanical conditions on neuromuscular coordination in stroke by testing the generalizability of muscle synergies after stroke between isometric force generation and free dynamic tasks. The results of this study provide valuable insights into the intermuscular coordination characteristics that both healthy individuals and stroke survivors adopt during various motor behaviors. Similar to our previous study with data collected from young healthy participants (23), neurologically intact, age-range-matched volunteers and stroke survivors showed the muscle synergy patterns shared between static and dynamic tasks, even though the EMG patterns differed across these two biomechanical conditions (Fig. 2). Moreover, we showed that altered, stroke-induced synergy patterns identified during both motor tasks could be explained as a linear combination of synergies identified from healthy individuals during the dynamic task. Our results also suggest that changes in the activation profile characteristics can vary between static and dynamic conditions. Overall, these findings provide evidence of the generalizability of within-subject intermuscular coordination patterns in the UE after stroke between static and free dynamic reaching, whereas their recruitment and modulation can differ across these two tasks. In addition, we discuss potential implications for developing novel rehabilitation strategies aimed at improving neuromuscular coordination after stroke.

The recruitment of muscle synergies during motor tasks reflects the adaptability and complexity of motor control (2, 29). Our findings indicate that healthy individuals recruited one more synergy during the dynamic reaching compared with the isometric force generation task, whereas stroke survivors tended to recruit a similar number of synergies across both tasks (Fig. 3). This limited synergy recruitment suggests a reduced ability to generate the complex motor patterns required for dynamic movements, potentially reflecting a diminished independence of neural control signals (30–32). For instance, a study showed that motor impairment was inversely related to the repertoire capacity of available muscle synergies, with fewer synergies observed in the arm of individuals after stroke (32). Therefore, developing novel rehabilitation strategies by aiming at expanding the repertoire of muscle synergies could improve motor function after stroke.

The within-subject similarity of muscle synergy patterns was comparable between isometric force generation and dynamic reaching tasks in both healthy and stroke conditions (Fig. 5), suggesting that the CNS might utilize neural mechanisms to control muscle activation shared across different tasks in both groups. The preservation of within-subject synergy composition across tasks is consistent with the concept of muscle synergy as a fundamental neuromuscular control mechanism for motor coordination. Furthermore, stroke survivors, particularly those with moderate to severe motor impairment, often exhibited altered, stroke-induced intermuscular coordination patterns across both motor tasks (Fig. 4). Similar to previous studies (29, 2), this finding suggests that atypical muscle synergy compositions remain and are recruited across varying biomechanical conditions, possibly indicating a fundamental aspect of post-stroke motor behavior. These persistent patterns of abnormal coordination underscore the need for rehabilitation strategies that target normalizing muscle synergy composition to potentially reduce motor impairment and improve activities of daily living after stroke.

Altered, stroke-induced intermuscular coordination patterns underlying both static and dynamic biomechanical conditions were largely explained by merging two out of the five available model synergies of healthy individuals identified during the dynamic task. This result demonstrates that abnormal muscle synergy patterns could be explained as a linear combination of two available model synergies, providing insight into the underlying neural mechanisms responsible for post-stroke motor deficits (17).

Even though the exact mechanism by which the CNS could orchestrate movement by activating motor modules remains unknown, previous studies have provided valuable insight. For example, many animal studies have shown that motor modules or muscle synergies are encoded in lower motor centers including the spinal cord or brainstem circuits (33–37).

One study with systematic neural transections in frogs has shown that most muscle synergies identified during natural complex movements, such as jumping or swimming, remain intact after the removal of supraspinal inputs (36). Additionally, a human study in healthy individuals provided neurophysiological evidence that the muscle synergies could be modulated at the cortical level and are not solely a product of the spinal circuitry by showing that specific motor cortical regions activate distinct muscle synergies (38). A recent lower extremity study found a phase-locked synchronization (coherence) between cortical activity and muscle synergy activation, and its modulation as a function of 30-min postural training, suggesting that the cortex is not only involved in initiating movement but also in dynamically modulating the recruitment of muscle synergies depending on the specific task demands (39). Collectively, the various possible locations within the CNS (e.g., the cortex, subcortical regions or spinal cord) and the mechanisms involved in synergy formation and recruitment are unlikely to be mutually exclusive, with each potentially contributing depending on the specific task requirements (40). Additionally, many studies have supported the idea that basic building blocks of motor control or muscle synergies could be preserved at the spinal or subcortical level after stroke, but the ability to selectively activate and combine these synergies is impaired due to disrupted descending cortical commands (27, 29, 41). These studies are consistent with our results that showed high similarity index values achieved through merging two model synergies of healthy individuals to explain the majority of the altered, stroke-induced synergies (Fig. 6). These results suggest that these abnormal synergy patterns could represent a maladaptive combination of pre-existing motor modules before stroke rather than the emergence of entirely new patterns. Thus, rehabilitation strategies that focus on fractionating these abnormal merged synergies by training how to individually control the model synergies of healthy individuals which constitute their merged patterns, could potentially improve motor coordination in stroke survivors (10, 42).

Although the majority of muscle synergy patterns are shared between isometric force generation and free dynamic reaching even in stroke survivors, the changes in the activation profile after stroke can vary depending on the biomechanical conditions. For instance, similar to our previous study (23), the averaged activation profiles in healthy individuals, in both the horizontal and frontal planes (Figs. 7 and 8, respectively), exhibited more directionally tuned synergy activation in the static condition than in the dynamic condition. However, the severely impaired stroke subgroup showed more tuned synergy activation in the dynamic condition than in the isometric condition. Furthermore, the average number of muscle synergies significantly activated across the 24 target directions was higher during the dynamic than static conditions for healthy individuals, whereas no significant difference was observed between the two tasks for mildly and moderately impaired stroke survivors (Fig. 9). Interestingly, the average number of muscle synergies significantly activated across the 24 targets was higher during isometric force generation than during point-to-point dynamic reaching tasks for the stroke subgroup with severe motor impairment. Therefore, further studies with a larger sample size in each stroke subgroup could investigate the mechanism underlying task-specific changes in the characteristics of synergy activation profiles across different levels of motor impairment. Overall, these results showed that the generalizability of muscle synergy after stroke is confine within the composition of motor modules, but the way stroke alters the activation profile might differ depending on the biomechanical conditions or level of motor impairment.

The correlation among all possible pairs of averaged synergy activation profiles within each healthy or stroke subgroup differed between isometric and dynamic biomechanical conditions in task performance (Fig. 10). This finding indicates that the recruitment of muscle synergies is task-dependent underlying different motor control strategies, as observed in previous studies (23, 43, 44). Furthermore, the sign and magnitude of the correlation of synergy activations across participant subgroups were largely consistent in the isometric task. However, during dynamic tasks, the sign and magnitude of the correlation differed across the four subgroups, particularly in the moderately and severely impaired stroke subgroups. This result suggests that while synergy recruitment strategies could be preserved under isometric conditions, the complexity of dynamic movement may induce disruptions in proper synergy recruitment in stroke. Interestingly, the severely impaired stroke subgroup exhibited abnormal positive coupling between the elbow flexor and shoulder extensor/abductor synergies during the dynamic task exclusively, a pattern consistent with the clinical flexor synergy (7, 45). Overall, these findings further emphasize that the dynamic condition, but not the isometric condition, can be suitable for revealing the nuance of motor deficits in the recruitment of muscle synergies in stroke.

There are several limitations in this study. First, in our previous study with data collected from young, healthy participants, the muscle synergy shared between isometric and dynamic conditions was observed across different starting arm positions within the horizontal plane that covers the UE workspace (23). In this study, two planes (horizontal and frontal) were included to increase the variability of the EMG data obtained in the 3D space for robust muscle synergy identification. However, only one starting arm position was selected because of time constraints. Future studies could investigate the generalizability of muscle synergy across different starting arm positions in stroke survivors. The second limitation is the use of linearized movement for the free dynamic task due to the design specification of the robotic device (KULSIS) adopted. Although no difference was observed between our findings in the age-range-matched control group, and our previous nonlinearized constraint study in young healthy individuals (23), whether these differences can be observed in stroke survivors is unclear. Indeed, a previous study showed that constrained movements induce slight but measurable changes in the composition and activation of muscle synergies after stroke compared with free-reaching tasks without any robotic device (46). The current study chose KULSIS for two main reasons: 1) to compare and contrast the isometric and dynamic conditions under the same postural constraints using the same robotic device, reducing the variability due to the use of different equipment; and 2) to include individuals with different level of motor impairment. Stroke survivors with moderate and severe motor impairment could not freely reach targets frequently using their impaired arm during unsupported conditions (47, 48). Third, the number of muscles included (n = 8) could be a limitation in translating the results to a larger set of muscles. Indeed, simulation and experimental studies have shown that both the number and the choice of muscles included in synergy analysis affect both the estimation of the number of synergies and their composition (49, 50). By increasing the number of muscles or selecting different muscles, future studies could address other clinically relevant patterns or compensatory movement strategies after stroke. Finally, another concern is the small sample size of stroke volunteers in each subgroup. A larger sample size would be needed to investigate the changes in the activation profile characteristics after stroke to test for significant differences not only between biomechanical conditions but also across the four subgroups (healthy individuals, and mildly, moderately and severely impaired stroke survivors).

These findings underscore the importance of considering the biomechanical conditions when new rehabilitation interventions are designed and highlight the potential of utilizing muscle synergy characteristics in a rehabilitative exercise design for stroke survivors. Dynamic reaching, which requires precise, multi-joint movement, is characterized by abnormal intermuscular coordination recruitment, yet not evident during isometric tasks. This finding supports the adoption of dynamic biomechanical conditions in a rehabilitation exercise design when the rehabilitation goal is to reduce the expression of pathological movement patterns such as the clinical flexor synergy. In contrast, isometric training could provide other advantages in neurorehabilitation, especially for individuals with severe motor impairments and for whom goal-directed reaching is unavailable. The relatively simpler motor mechanisms involved in isometric force generation, evidenced by its intrinsic characteristic of static muscle contractions without joint movement as well as by a more preserved correlation between pairs of synergy activation profiles, suggests that isometric biomechanical conditions would be more accessible in early rehabilitation phases. For instance, previous studies have shown that stroke survivors can experience joint contracture and a reduced range of motion in the UE (51, 52), particularly during the early stages of rehabilitation; thus, static rehabilitation could be an alternative effective rehabilitation strategy during this period. Furthermore, the evidence of shared muscle synergies between isometric force generation and dynamic reaching suggests that improvements in intermuscular coordination achieved during isometric training could translate to enhanced performance of functional dynamic reaching, and vice versa. Therefore, isometric exercises could serve as a valuable therapeutic foundation for promoting neuromuscular recovery and potentially restoring coordination across a broader range of motor behaviors. Overall, these results contribute to understanding the abnormalities in stroke-induced intermuscular coordination under varying biomechanical conditions and could be translated into developing novel and more effective neurorehabilitation interventions for post-stroke motor recovery.

Abbreviations

Declarations

Ethics approval and consent to participate

This study followed the guidelines of the Declaration of Helsinki, with the approval of the University of Houston Institutional Review Board. All participants provided informed written consent before the beginning of the study.

Availability of data and materials

The data used in this study might be available from the corresponding author upon a reasonable request.

Competing interests

The authors declare that they have no known competing financial interests or personal relationships that could have appeared to influence the work reported in this paper.

Funding

This study was supported by the National Science Foundation (Award ID: 2145321 to Roh).

Authors' contributions

MPJ: Study Design, Data collection, Data analysis, Writing – original draft, Writing – review and editing. **YNGH:** Study Design, Data collection, Data analysis, Writing – review and editing. **KK:** Clinical Assessment, Writing – review and editing. **H-SP**, **SL**, and **JR:** Conceptualization, Writing – review and editing. **JR:** Study Design, Original Idea. All authors read and approved the final manuscript.

References

- 1. Lin DJ, Hardstone R, DiCarlo JA, Mckiernan S, Snider SB, Jacobs H, et al. Distinguishing Distinct Neural Systems for Proximal vs Distal Upper Extremity Motor Control After Acute Stroke. Neurology. 2023 Jul 25;101(4):e347–57.
- 2. Zhao K, He C, Xiang W, Zhou Y, Zhang Z, Li J, et al. Evidence of synergy coordination patterns of upper-limb motor control in stroke patients with mild and moderate impairment. Front Physiol. 2023;14:1214995.
- 3. Tresch MC, Jarc A. The case for and against muscle synergies. Curr Opin Neurobiol. 2009 Dec 1;19(6):601-7.
- 4. Roh J, Rymer WZ, Beer RF. Robustness of muscle synergies underlying three-dimensional force generation at the hand in healthy humans. J Neurophysiol. 2012 Apr 15;107(8):2123–42.
- 5. Bizzi E, Cheung VC. The neural origin of muscle synergies. Front Comput Neurosci [Internet]. 2013 Apr 29 [cited 2025 Jun 2];7. Available from: https://www.frontiersin.org/journals/computational-neuroscience/articles/10.3389/fncom.2013.00051/full
- 6. Roh J, Lee ,Sang Wook, and Wilger KD. Modular Organization of Exploratory Force Development Under Isometric Conditions in the Human Arm. J Mot Behav. 2019 Jan 2;51(1):83–99.
- 7. Twitchell TE. The restoration of motor function following hemiplegia in man. Brain. 1951 Dec 1;74(4):443-80.
- 8. McPherson LM, Dewald JPA. Differences between flexion and extension synergy-driven coupling at the elbow, wrist, and fingers of individuals with chronic hemiparetic stroke. Clin Neurophysiol Off J Int Fed Clin Neurophysiol. 2019 Apr;130(4):454–68.
- 9. Roh J, Rymer WZ, Perreault EJ, Yoo SB, Beer RF. Alterations in upper limb muscle synergy structure in chronic stroke survivors. J Neurophysiol. 2013 Feb;109(3):768–81.
- 10. Park JH, Shin JH, Lee H, Roh J, Park HS. Relevance of Upper Limb Muscle Synergies to Dynamic Force Generation: Perspectives on Rehabilitation of Impaired Intermuscular Coordination in Stroke. IEEE Trans Neural Syst Rehabil Eng

- Publ IEEE Eng Med Biol Soc. 2023;31:4851-61.
- 11. Facciorusso S, Guanziroli E, Brambilla C, Spina S, Giraud M, Molinari Tosatti L, et al. Muscle synergies in upper limb stroke rehabilitation: a scoping review. Eur J Phys Rehabil Med. 2024 Oct;60(5):767–92.
- 12. Portilla-Jiménez M, Seo G, Houston M, Hong YNG, Li S, Park HS, et al. Muscle Synergy-Guided Exercise Through Human-Machine Interaction Can Improve Neuromuscular Coordination and Decrease Motor Impairment After Stroke: A Pilot Study. In: Pons JL, Tornero J, Akay M, editors. Converging Clinical and Engineering Research on Neurorehabilitation V. Cham: Springer Nature Switzerland; 2025. p. 362–6.
- 13. Seo G, Houston M, Portilla M, Fang F, Park JH, Lee H, et al. Expanding the repertoire of intermuscular coordination patterns and modulating intermuscular connectivity in stroke-affected upper extremity through electromyogram-guided training: a pilot study. In: 2023 45th Annual International Conference of the IEEE Engineering in Medicine & Biology Society (EMBC) [Internet]. 2023 [cited 2025 Jun 5]. p. 1–4. Available from: https://ieeexplore.ieee.org/abstract/document/10341085
- 14. Portilla-Jiménez M, Seo G, Houston M, Hong YNG, Li S, Park HS, et al. Improving impaired intermuscular coordination after stroke through synergy-guided human-machine interaction: a pilot study. In: 2024 46th Annual International Conference of the IEEE Engineering in Medicine and Biology Society (EMBC) [Internet]. 2024 [cited 2025 Jun 19]. p. 1–4. Available from: https://ieeexplore.ieee.org/abstract/document/10782001
- 15. Ferrante S, Chia Bejarano N, Ambrosini E, Nardone A, Turcato AM, Monticone M, et al. A Personalized Multi-Channel FES Controller Based on Muscle Synergies to Support Gait Rehabilitation after Stroke. Front Neurosci [Internet]. 2016 Sep 16 [cited 2025 Jun 5];10. Available from: https://www.frontiersin.org/journals/neuroscience/articles/10.3389/fnins.2016.00425/full
- 16. Niu CM, Bao Y, Zhuang C, Li S, Wang T, Cui L, et al. Synergy-Based FES for Post-Stroke Rehabilitation of Upper-Limb Motor Functions. IEEE Trans Neural Syst Rehabil Eng. 2019 Feb;27(2):256–64.
- 17. Israely S, Leisman G, Carmeli E. Neuromuscular synergies in motor control in normal and poststroke individuals. Rev Neurosci. 2018 Aug 28;29(6):593–612.
- 18. McMorland AJC, Runnalls KD, Byblow WD. A neuroanatomical framework for upper limb synergies after stroke. Front Hum Neurosci. 2015;9:82.
- 19. Roh J, Rymer WZ, Beer RF. Evidence for altered upper extremity muscle synergies in chronic stroke survivors with mild and moderate impairment. Front Hum Neurosci [Internet]. 2015 Feb 11 [cited 2025 Mar 20];9. Available from: https://www.frontiersin.org/journals/human-neuroscience/articles/10.3389/fnhum.2015.00006/full
- 20. Li S, Zhuang C, Niu CM, Bao Y, Xie Q, Lan N. Evaluation of Functional Correlation of Task-Specific Muscle Synergies with Motor Performance in Patients Poststroke. Front Neurol. 2017;8:337.
- 21. Pan B, Sun Y, Xie B, Huang Z, Wu J, Hou J, et al. Alterations of Muscle Synergies During Voluntary Arm Reaching Movement in Subacute Stroke Survivors at Different Levels of Impairment. Front Comput Neurosci. 2018;12:69.
- 22. Park JH, Shin JH, Lee H, Roh J, Park HS. Alterations in intermuscular coordination underlying isokinetic exercise after a stroke and their implications on neurorehabilitation. J Neuroengineering Rehabil. 2021 Jul 3;18(1):110.
- 23. Pham K, Portilla-Jiménez M, Roh J. Generalizability of muscle synergies in isometric force generation versus point-to-point reaching in the human upper extremity workspace. Front Hum Neurosci [Internet]. 2023 Jul 17 [cited 2025 Apr 12];17. Available from: https://www.frontiersin.org/turnals/human-neuroscience/articles/10.3389/fnhum.2023.1144860/full
- 24. Ambrosini E, De Marchis C, Pedrocchi A, Ferrigno G, Monticone M, Schmid M, et al. Neuro-Mechanics of Recumbent Leg Cycling in Post-Acute Stroke Patients. Ann Biomed Eng. 2016 Nov 1;44(11):3238–51.
- 25. Park JH, Shin JH, Lee H, Park CB, Roh J, Park HS. Design and Evaluation of a Novel Experimental Setup for Upper Limb Intermuscular Coordination Studies. Front Neurorobotics [Internet]. 2019 Sep 6 [cited 2025 Apr 13];13. Available from: https://www.frontiersin.org/tournals/neurorobotics/articles/10.3389/fnbot.2019.00072/full

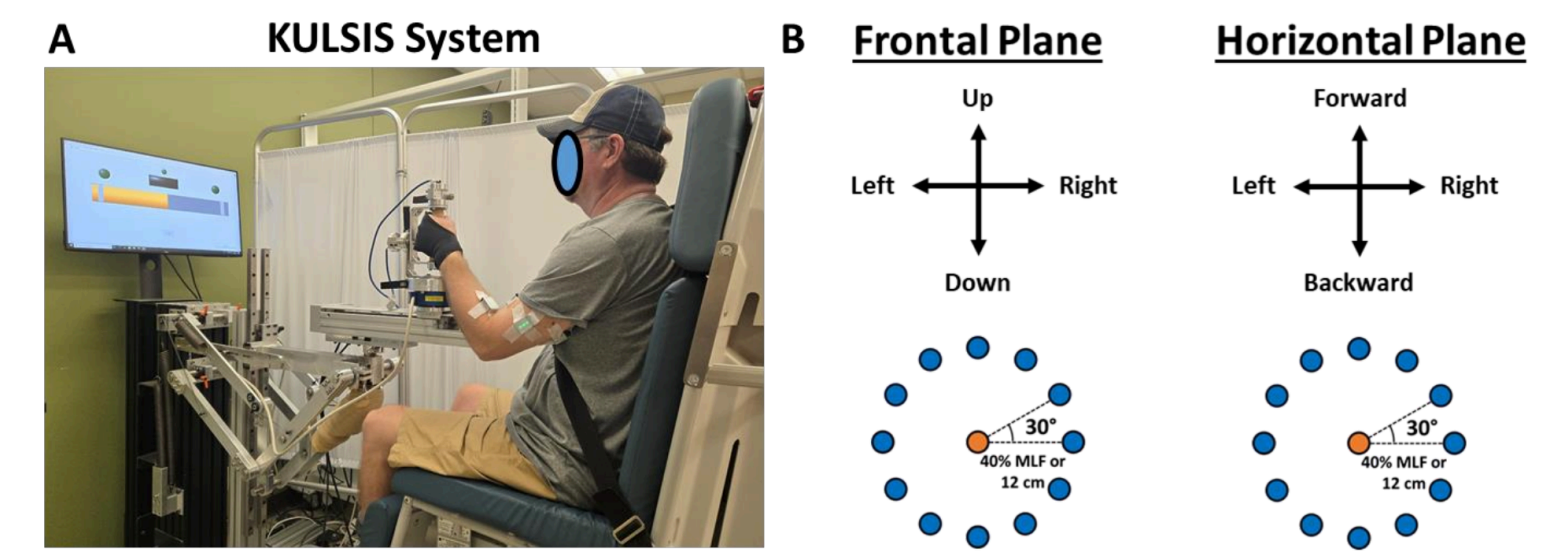
- 26. Seo G, Lee SW, Beer RF, Alamri A, Wu YN, Raghavan P, et al. Alterations in motor modules and their contribution to limitations in force control in the upper extremity after stroke. Front Hum Neurosci [Internet]. 2022 Jul 28 [cited 2025 Apr 12];16. Available from: https://www.frontiersin.org/https://www.frontiersin.org/journals/human-neuroscience/articles/10.3389/fnhum.2022.937391/full
- 27. Cheung VCK, Turolla A, Agostini M, Silvoni S, Bennis C, Kasi P, et al. Muscle synergy patterns as physiological markers of motor cortical damage. Proc Natl Acad Sci U S A. 2012 Sep 4;109(36):14652–6.
- 28. Barroso FO, Torricelli D, Moreno JC, Taylor J, Gomez-Soriano J, Bravo-Esteban E, et al. Shared muscle synergies in human walking and cycling. J Neurophysiol. 2014 Oct 15;112(8):1984–98.
- 29. Cheung VCK, Piron L, Agostini M, Silvoni S, Turolla A, Bizzi E. Stability of muscle synergies for voluntary actions after cortical stroke in humans. Proc Natl Acad Sci. 2009 Nov 17;106(46):19563–8.
- 30. Mehrabi N, Schwartz MH, Steele KM. Can altered muscle synergies control unimpaired gait? J Biomech. 2019 Jun 11:90:84–91.
- 31. Kuska EC, Mehrabi N, Schwartz MH, Steele KM. Number of synergies impacts sensitivity of gait to weakness and contracture. J Biomech. 2022 Mar;134:111012.
- 32. Ortega-Auriol P, Byblow WD, Ren AX, Besier T, McMorland AJC. The role of muscle synergies and task constraints on upper limb motor impairment after stroke. Exp Brain Res. 2025 Jan 8;243(1):40.
- 33. Bizzi E, Cheung VCK, d'Avella A, Saltiel P, Tresch M. Combining modules for movement. Brain Res Rev. 2008 Jan 1;57(1):125–33.
- 34. Desrochers E, Harnie J, Doelman A, Hurteau MF, Frigon A. Spinal control of muscle synergies for adult mammalian locomotion. J Physiol. 2019 Jan;597(1):333–50.
- 35. Klishko AN, Harnie J, Hanson CE, Rahmati SM, Rybak IA, Frigon A, et al. Effects of spinal transection and locomotor speed on muscle synergies of the cat hindlimb. J Physiol. 2025 May;603(10):3061–88.
- 36. Roh J, Cheung VCK, Bizzi E. Modules in the brain stem and spinal cord underlying motor behaviors. J Neurophysiol. 2011 Sep;106(3):1363–78.
- 37. Tresch MC, Bizzi E. Responses to spinal microstimulation in the chronically spinalized rat and their relationship to spinal systems activated by low threshold cutaneous stimulation. Exp Brain Res. 1999 Nov 1;129(3):401–16.
- 38. Rana M, Yani MS, Asavasopon S, Fisher BE, Kutch JJ. Brain Connectivity Associated with Muscle Synergies in Humans. J Neurosci. 2015 Nov 4;35(44):14708–16.
- 39. Zandvoort CS, van Dieën JH, Dominici N, Daffertshofer A. The human sensorimotor cortex fosters muscle synergies through cortico-synergy coherence. NeuroImage. 2019 Oct 1;199:30–7.
- 40. McMorland AJC, Runnalls KD, Byblow WD. A Neuroanatomical Framework for Upper Limb Synergies after Stroke. Front Hum Neurosci. 2015 Feb 16;9:82.
- 41. McPherson LM, Dewald JPA. Abnormal synergies and associated reactions post-hemiparetic stroke reflect muscle activation patterns of brainstem motor pathways. Front Neurol. 2022;13:934670.
- 42. Mizuta N, Hasui N, Nishi Y, Higa Y, Matsunaga A, Deguchi J, et al. Merged swing-muscle synergies and their relation to walking characteristics in subacute post-stroke patients: An observational study. PloS One. 2022;17(2):e0263613.
- 43. Brambilla C, Atzori M, Müller H, d'Avella A, Scano A. Spatial and Temporal Muscle Synergies Provide a Dual Characterization of Low-dimensional and Intermittent Control of Upper-limb Movements. Neuroscience. 2023 Mar 15;514:100–22.
- 44. Chen X, Dong X, Feng Y, Jiao Y, Yu J, Song Y, et al. Muscle activation patterns and muscle synergies reflect different modes of coordination during upper extremity movement. Front Hum Neurosci. 2022;16:912440.
- 45. McPherson JG, Chen A, Ellis MD, Yao J, Heckman CJ, Dewald JPA. Progressive recruitment of contralesional corticoreticulospinal pathways drives motor impairment post stroke. J Physiol. 2018 Apr 1;596(7):1211–25.

- 46. Scano A, Chiavenna A, Malosio M, Molinari Tosatti L, Molteni F. Robotic Assistance for Upper Limbs May Induce Slight Changes in Motor Modules Compared With Free Movements in Stroke Survivors: A Cluster-Based Muscle Synergy Analysis. Front Hum Neurosci. 2018;12:290.
- 47. Williams MR. A pilot study into reaching performance after severe to moderate stroke using upper arm support. PloS One. 2018;13(7):e0200787.
- 48. Runnalls KD, Ortega-Auriol P, McMorland AJC, Anson G, Byblow WD. Effects of arm weight support on neuromuscular activation during reaching in chronic stroke patients. Exp Brain Res. 2019 Dec;237(12):3391–408.
- 49. Steele KM, Tresch MC, Perreault EJ. The number and choice of muscles impact the results of muscle synergy analyses. Front Comput Neurosci. 2013;7:105.
- 50. Brambilla C, Scano A. The Number and Structure of Muscle Synergies Depend on the Number of Recorded Muscles: A Pilot Simulation Study with OpenSim. Sensors. 2022 Nov 8;22(22):8584.
- 51. Sackley C, Brittle N, Patel S, Ellins J, Scott M, Wright C, et al. The prevalence of joint contractures, pressure sores, painful shoulder, other pain, falls, and depression in the year after a severely disabling stroke. Stroke. 2008 Dec;39(12):3329–34.
- 52. Matozinho CVO, Teixeira-Salmela LF, Samora GAR, Sant'Anna R, Faria CDCM, Scianni A. Incidence and potential predictors of early onset of upper-limb contractures after stroke. Disabil Rehabil. 2021 Mar;43(5):678–84.

Table 1

Table 1 is available in the Supplementary Files section.

Figures



C Six Rail Positions for the Dynamic Task

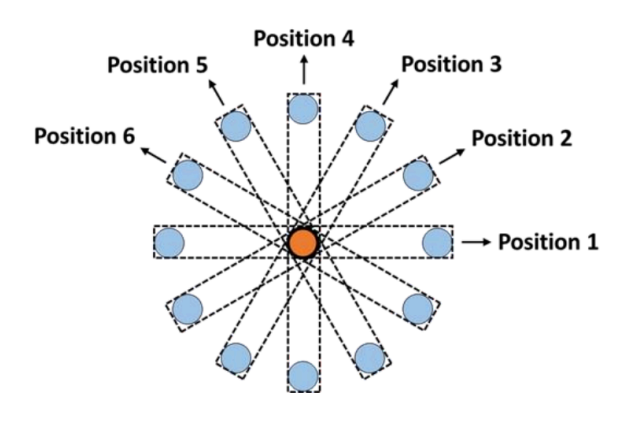


Figure 1

Experimental setup. A, the KULSIS system was used for isometric force generation and free reaching tasks. The participants grabbed the end-effector of the device, the handle, connected to a load cell to measure the force. During the isometric task, participants applied force without moving the handle, while participants linearly moved the handle location through the rail during free reaching. B, the 24 targets (blue circles) defined in the horizontal and frontal planes were equally distributed around the starting arm location (orange circles). For the isometric force generation task, the target force magnitude was set as 40% of the maximum lateral force (MLF). In addition, the 3D forces and directions were defined as follows: in the horizontal plane, lateral (+Fx), medial (-Fx), forward (+Fy), and backward (-Fy), while in the frontal plane the system was rotated, resulting in lateral (+Fx), medial (-Fx), up (+Fy) and down (-Fy). For the dynamic reaching task, the center-out reaching distance to match the target was a location within 10 to 12 cm. During both tasks, for participants whose left-arm data were collected, medial and lateral data were flipped to match the right-handed orientation during data processing. C, for the dynamic task, the rail was manually rotated into one of the six predefined positions, which were evenly spaced within each plane (horizontal or frontal) to guide the reaching movement. For each rail orientation, participants performed center-out reaches from the starting arm location (marked by the orange circle) toward one of the two randomized targets (soft blue circles). For example, in position 1, the target directions available were medial and lateral.

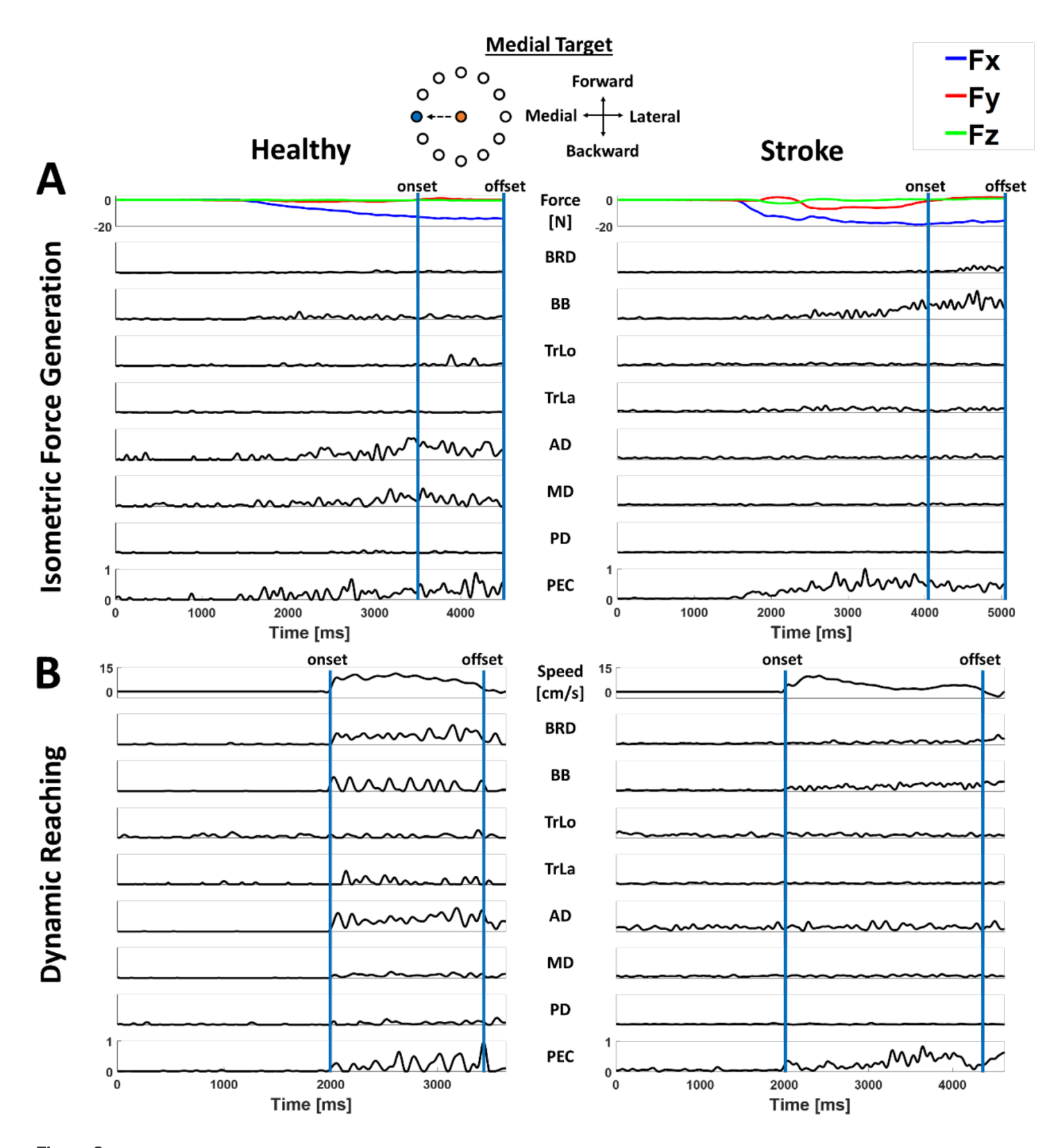


Figure 2

Representative EMG, force, and speed data were collected from one healthy participant (left) and one post-stroke volunteer (right) for both isometric force production and dynamic reaching tasks. EMG signals were collected during center-out, point-to-point reaching under static or dynamic conditions to the nine-o'clock direction. The signals were normalized for each muscle against the maximum contraction observed across all trials within each motor task for visualization to highlight muscle activation patterns throughout the trial. **A**, three-dimensional endpoint forces (Fx, lateral-medial; Fy, forward-backward; Fz, upward-downward) and EMG signals were recorded during the isometric force target-matching task.

The one-second holding period data, demarcated by the two blue lines, were used for synergy analysis. **B**, Hand speed and EMG activity during a center-out reaching movement. EMG data from the movement onset to offset based on the 10% of max speed (indicated by the blue lines) were included for synergy identification. The muscles recorded were brachioradialis (BRD), biceps brachii (BB), triceps brachii (long and lateral heads) (TrLo and TrLa, respectively), deltoids (anterior, middle, and posterior fibers; AD, MD, and PD, respectively), and pectoralis major clavicular head (PEC).

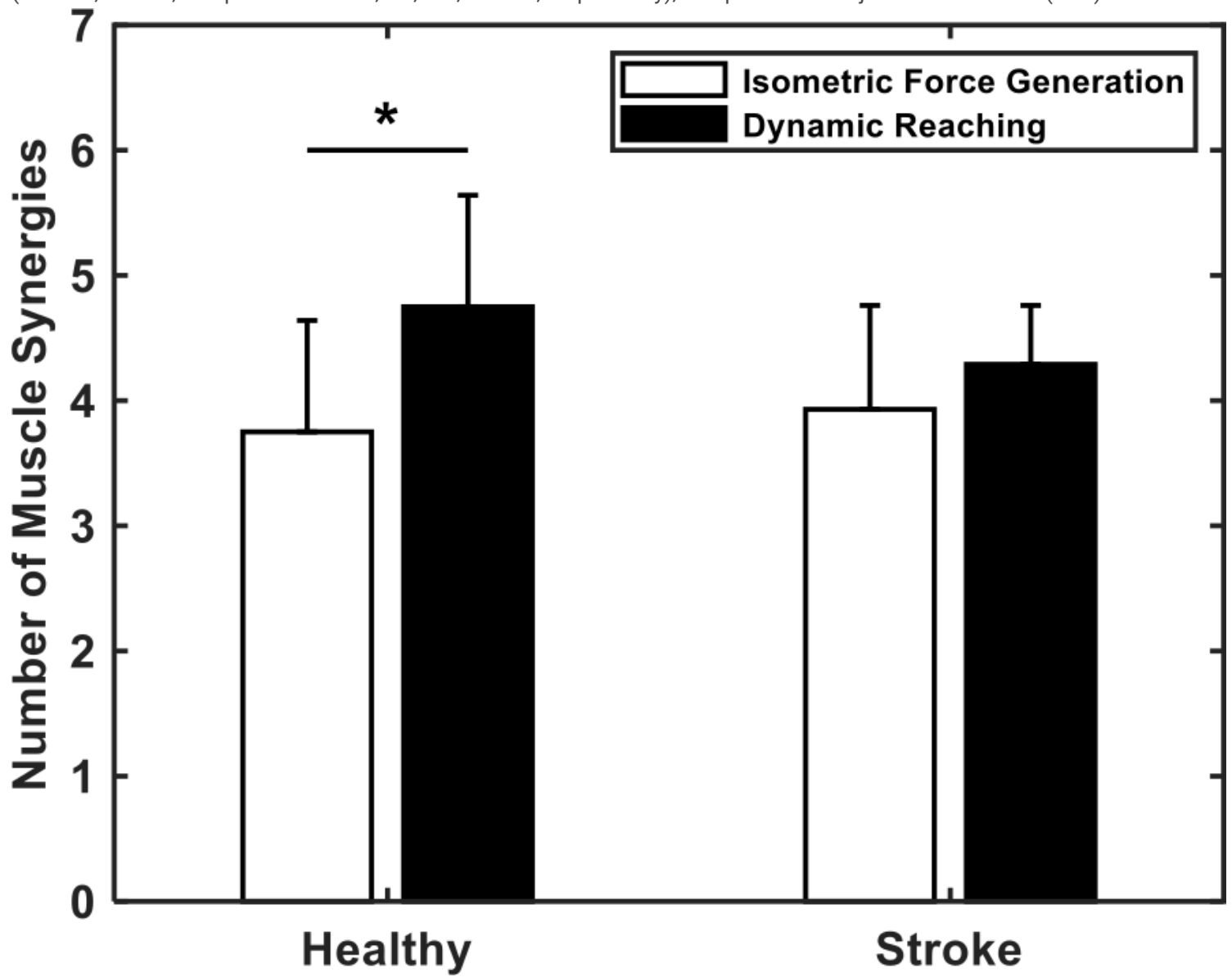


Figure 3

The optimal number of muscle synergies (mean \pm SD) during isometric force generation (white) and dynamic reaching (black) tasks for the healthy individuals (n = 8) and stroke survivors (n = 14). The criteria for the optimal number of muscle synergies per participant included 90% of the global variance accounted for (gVAF) and a 5% difference of gVAF by adding one more synergy (diffVAF; see Method section, Muscle Synergy Identification). There was a significant difference between the isometric force generation and dynamic reaching tasks in the healthy group exclusively (paired t-test; *, p < 0.05).

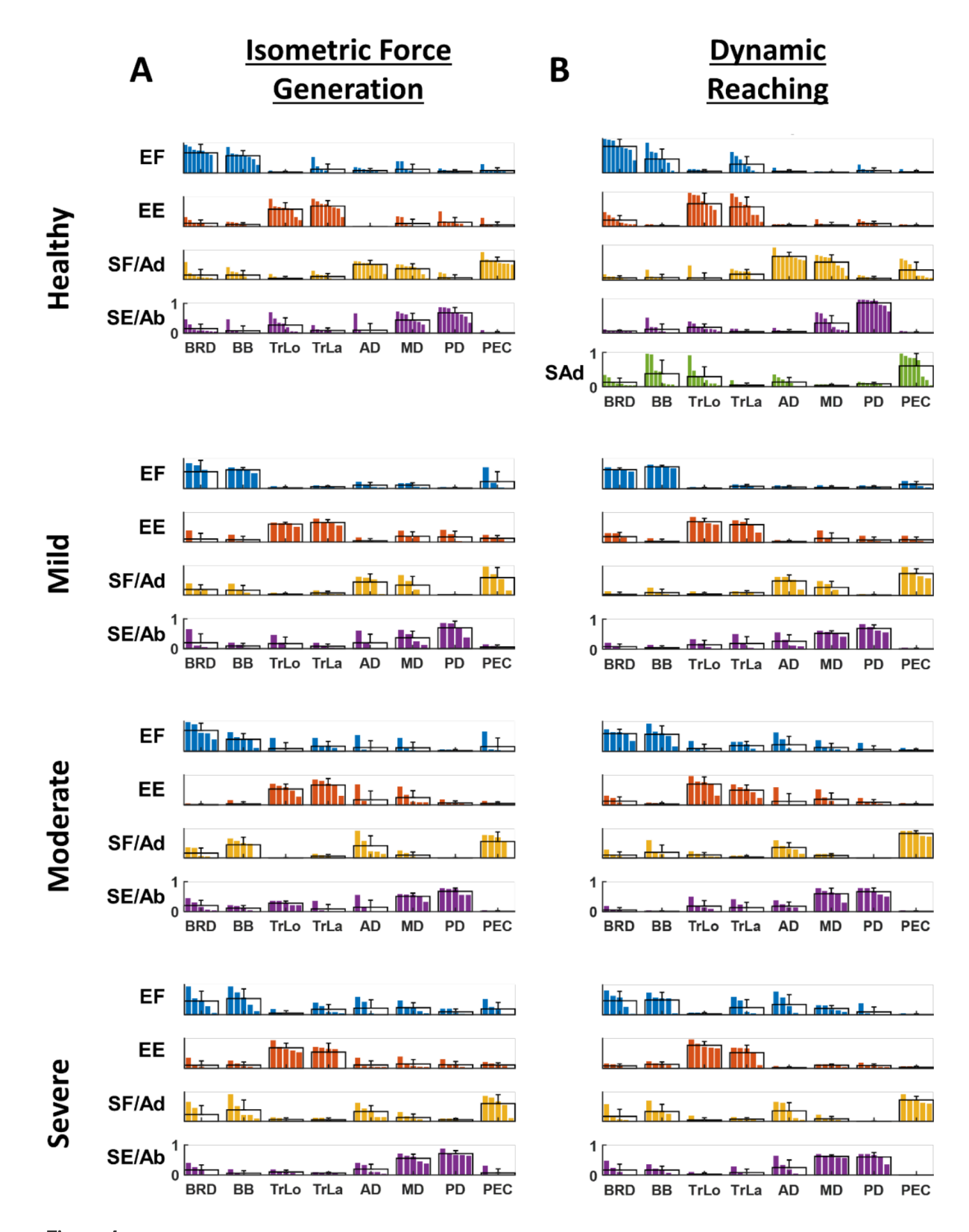


Figure 4

Muscle synergy patterns (EF, elbow flexor; EE, elbow extensor; SF/Ad, shoulder flexor/adductor; SE/Ab, shoulder extensor/abductor; and SAd, shoulder adductor) per subgroup (n = 8, healthy; n = 4, mild; n = 5, moderate; and n = 5, severe) during isometric force generation (**A**) and dynamic reaching (**B**). SAd synergy was identified exclusively in the healthy group during the dynamic condition. The muscle synergy composition was consistent with some small variations within each of the four subgroups. Nevertheless, group differences were observed, especially in EF and SF/Ad for moderately and severely impaired stroke subgroups compared with healthy individuals or mildly impaired participants.

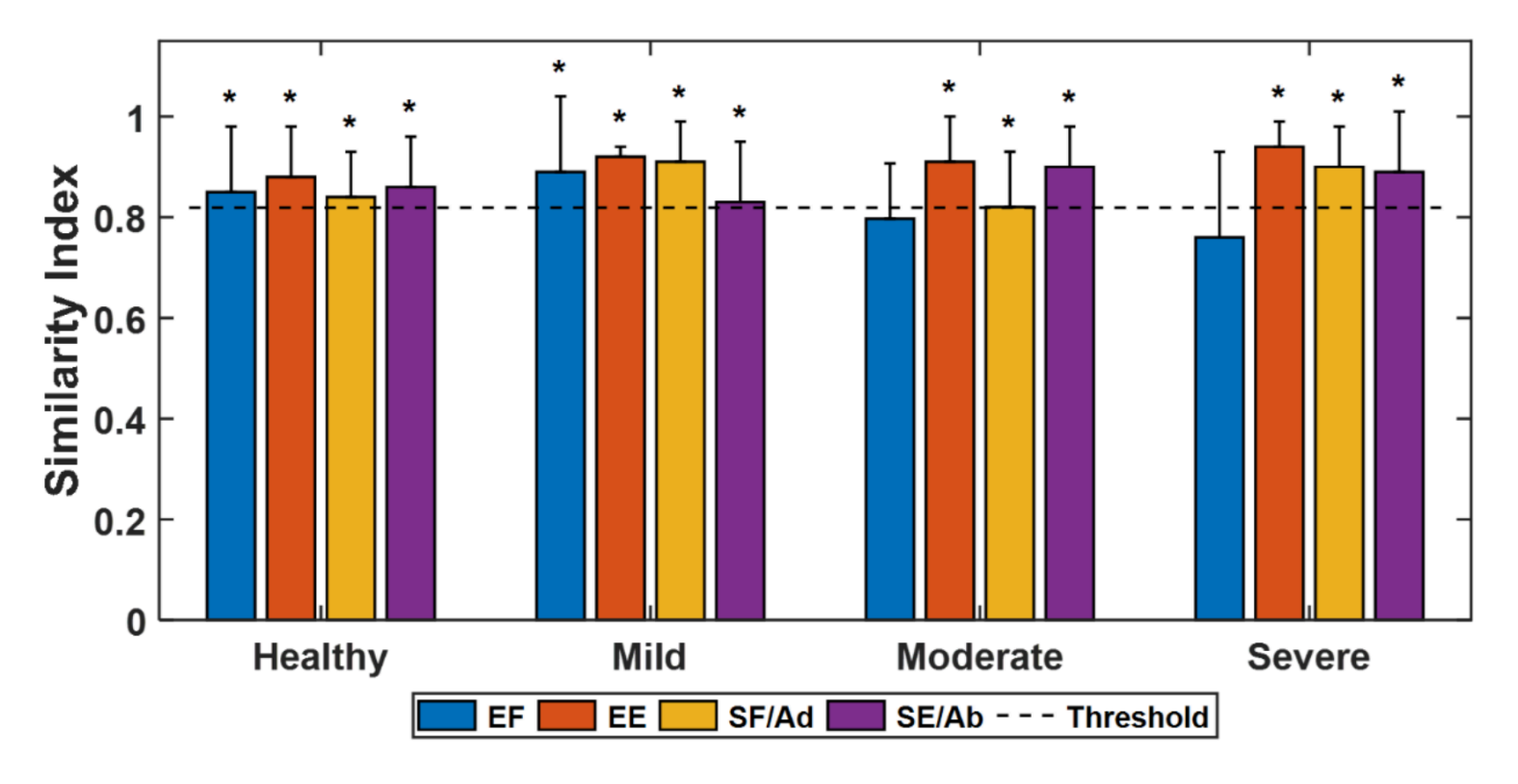


Figure 5

Muscle synergy composition similarity between isometric force generation and dynamic reaching within each group. Four pairs of synergies (EF, elbow flexor; EE, elbow extensor; SF/Ad, shoulder flexor/adductor; SE/Ab, shoulder extensor/abductor) underlying the two tasks were similar (*, p < 0.05) within each participant in the healthy and mildly impaired stroke groups. Three pairs of synergies (EE, SF/Ad, and SE/Ab) were similar between the static and dynamic tasks for the moderately and severely impaired stroke groups. The dotted line indicates the statistical threshold.

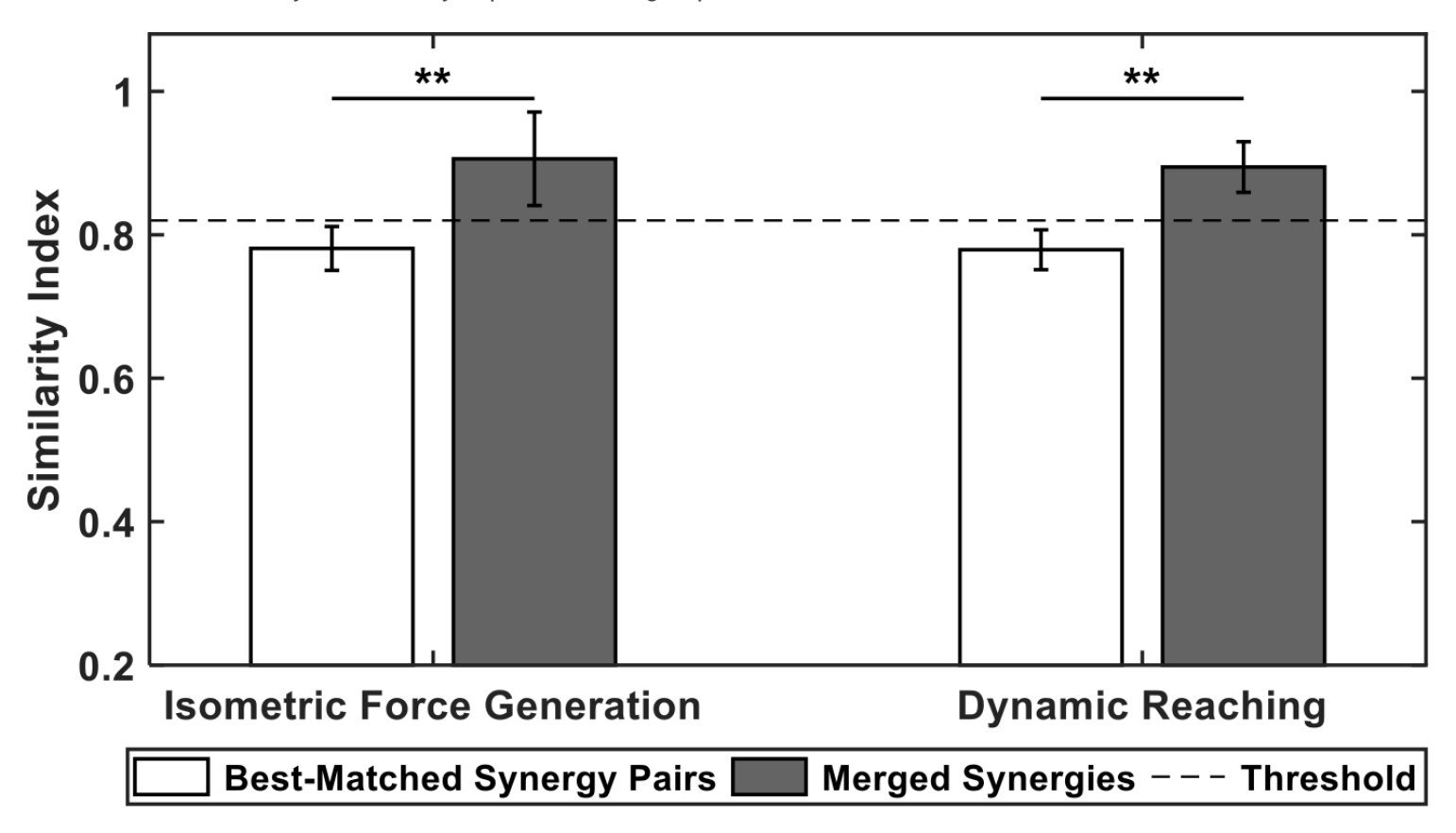


Figure 6

The altered, stroke-induced synergies were explained by merging the model muscle synergies underlying the dynamic reaching from the healthy individuals. The two white bars represent the similarity index (mean \pm SD) of the scalar product of the best-matched synergy pairs between each altered, stroke-induced synergy and the norm synergies (i.e., the averaged synergies within the healthy group) underlying dynamic reaching. The two gray bars show the similarity between altered, stroke-induced synergies and the merging of two norm synergies during the dynamic task, which are higher than the first two, respectively (***, p < 0.01). The dashed line shows the statistical threshold of the similarity index. Altered synergies that were explained by merging model synergies of healthy individuals were included exclusively (n = 9, isometric force generation; and n = 12, dynamic reaching).

Horizontal Plane

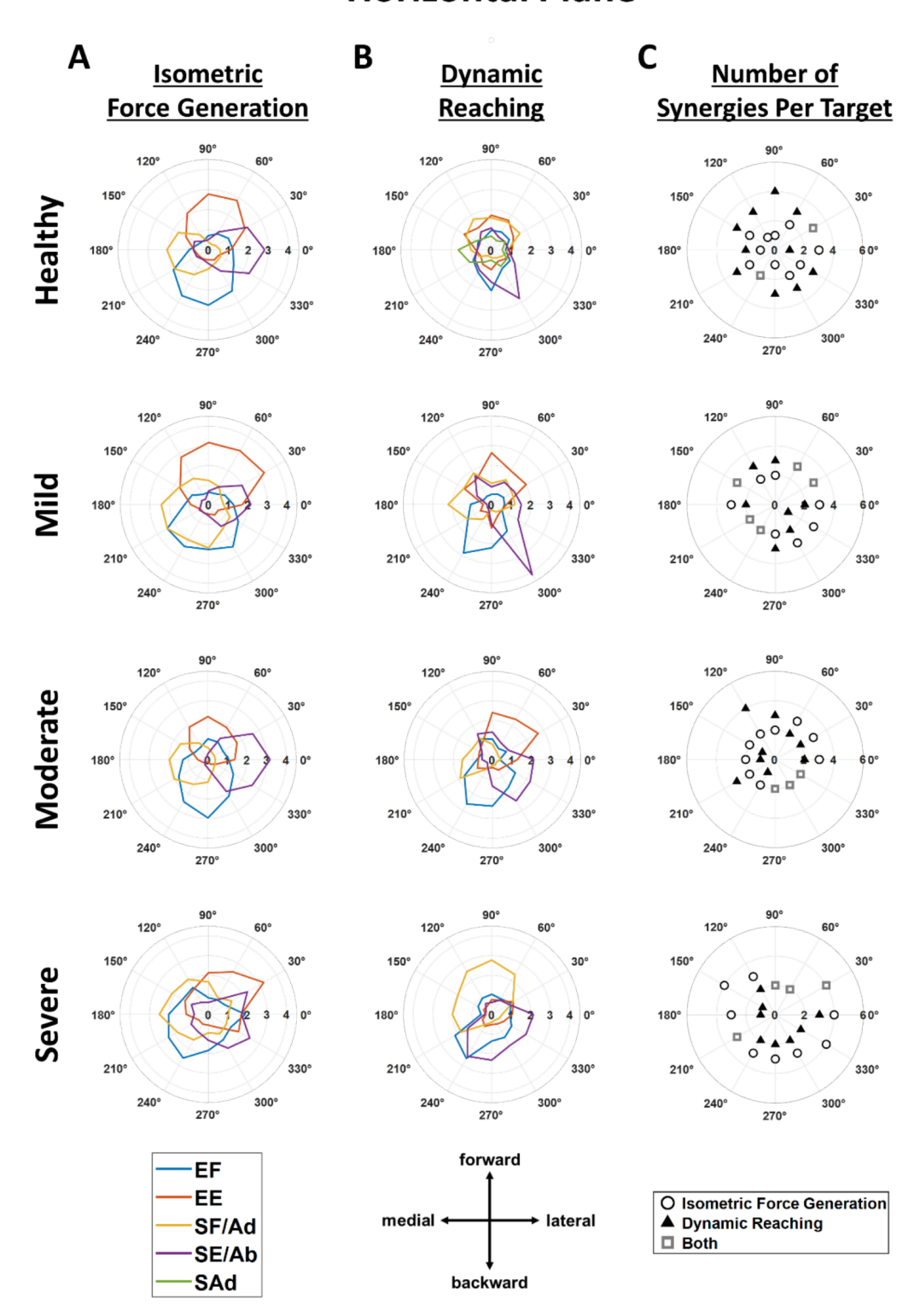


Figure 7

The averaged tuning curves of muscle synergy activation and the number of significantly activated synergies per target direction during isometric force generation (**A**) and dynamic reaching (**B**) in the horizontal plane per subgroup. The muscle synergy activation tuning curves were more tuned during isometric force generation than during dynamic reaching for all subgroups, except the severely impaired stroke subgroup. Each of the five colors is mapped to each of the five synergy-activation profiles. **C**, the number of muscle synergies significantly activated across the 12 target directions in the isometric force generation (circle) and dynamic reaching (triangle) based on the mean muscle synergy activation per

subgroup. The squares refer to the case in which the number of significantly activated synergies is the same for both tasks in a specific target direction. The magnitude of the mean synergy activation greater than the threshold (see **Method section**, Number of synergies required per target direction) was considered significant. For the healthy group, the number of synergies significantly activated per target direction was typically lower in the isometric force generation than in the dynamic reaching. In contrast, for the severely impaired stroke subgroup, the number of synergies was typically higher in the isometric task than in the dynamic task. For the mildly and moderately impaired stroke subgroups, no clear difference between conditions was observed. EF, elbow flexor; EE, elbow extensor; SF/Ad, shoulder flexor/adductor; SE/Ab, shoulder extensor/abductor; and SAd, shoulder adductor.

Frontal Plane

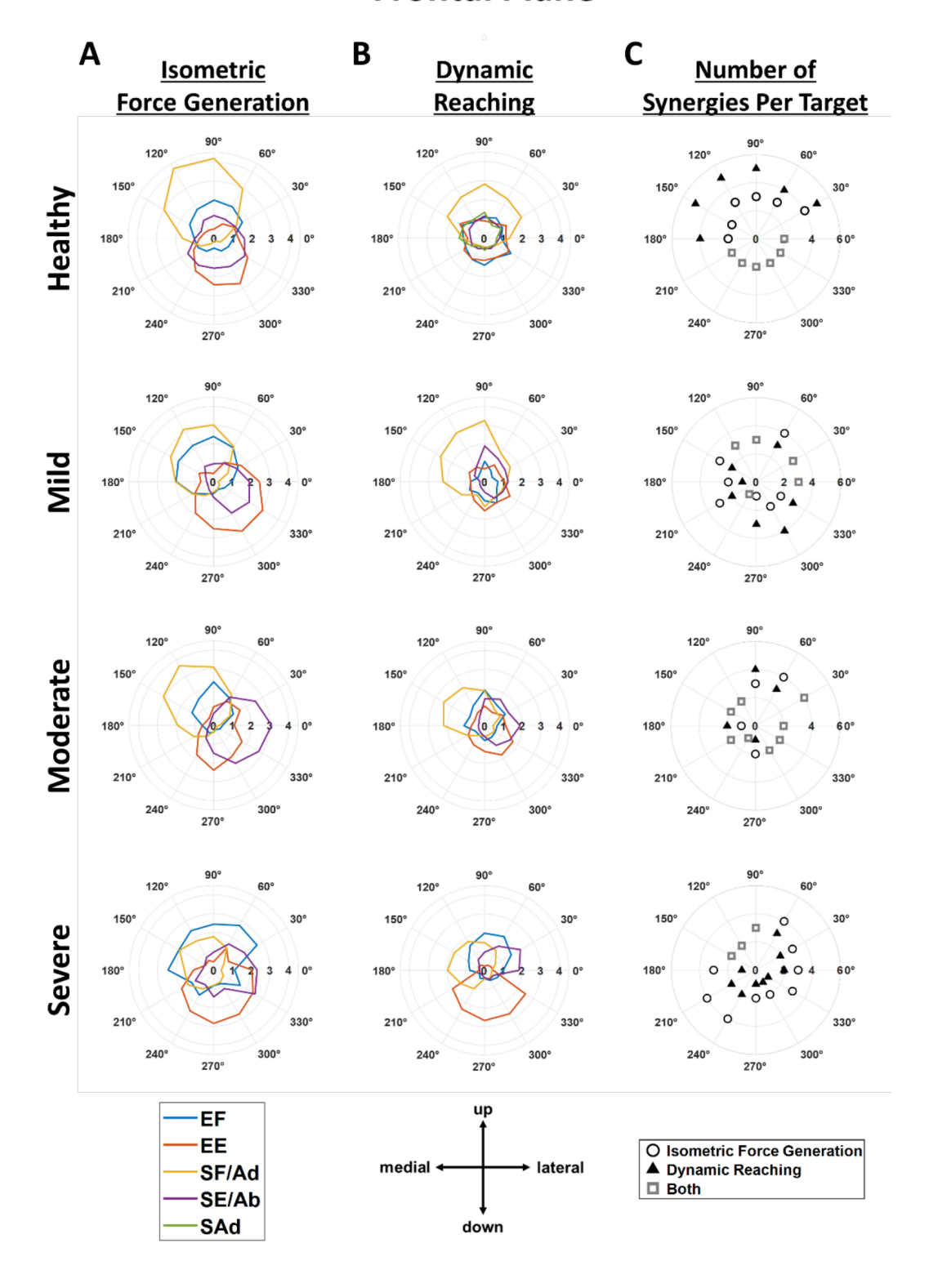


Figure 8

The averaged tuning curves of muscle synergy activation profiles and the number of significantly activated synergies per target direction during static (A) and dynamic (B) tasks in the frontal plane, across subgroups. In general, synergy activation tuning curves were more tuned during static than during dynamic reaching for healthy individuals, and mildly, and moderately impaired stroke survivors, but not for the severely impaired stroke subgroup. Each of the five colors from the activation tuning curve is mapped to each of the five muscle synergy activation profiles. C, the number of significantly activated muscle synergies across the 12 target directions for both tasks (circles indicate isometric force generation, triangles indicate dynamic reaching, and squares represent target directions where participants activated the same number of synergies in both tasks). Synergy activation was considered significant if its average magnitude exceeded a defined threshold (see Method section, Number of synergies required per target direction). For healthy individuals, fewer synergies per target direction were typically activated during isometric force generation than during dynamic reaching. Conversely, for stroke survivors with severe motor impairment, the number of synergies was typically higher in the isometric task than in the point-to-point reaching task. No consistent difference in the number of activated synergies was observed between the two tasks in the mildly and moderately impaired stroke subgroups. EF, elbow flexor; EE, elbow extensor; SF/Ad, shoulder flexor/adductor; SE/Ab, shoulder extensor/abductor; and SAd, shoulder adductor.

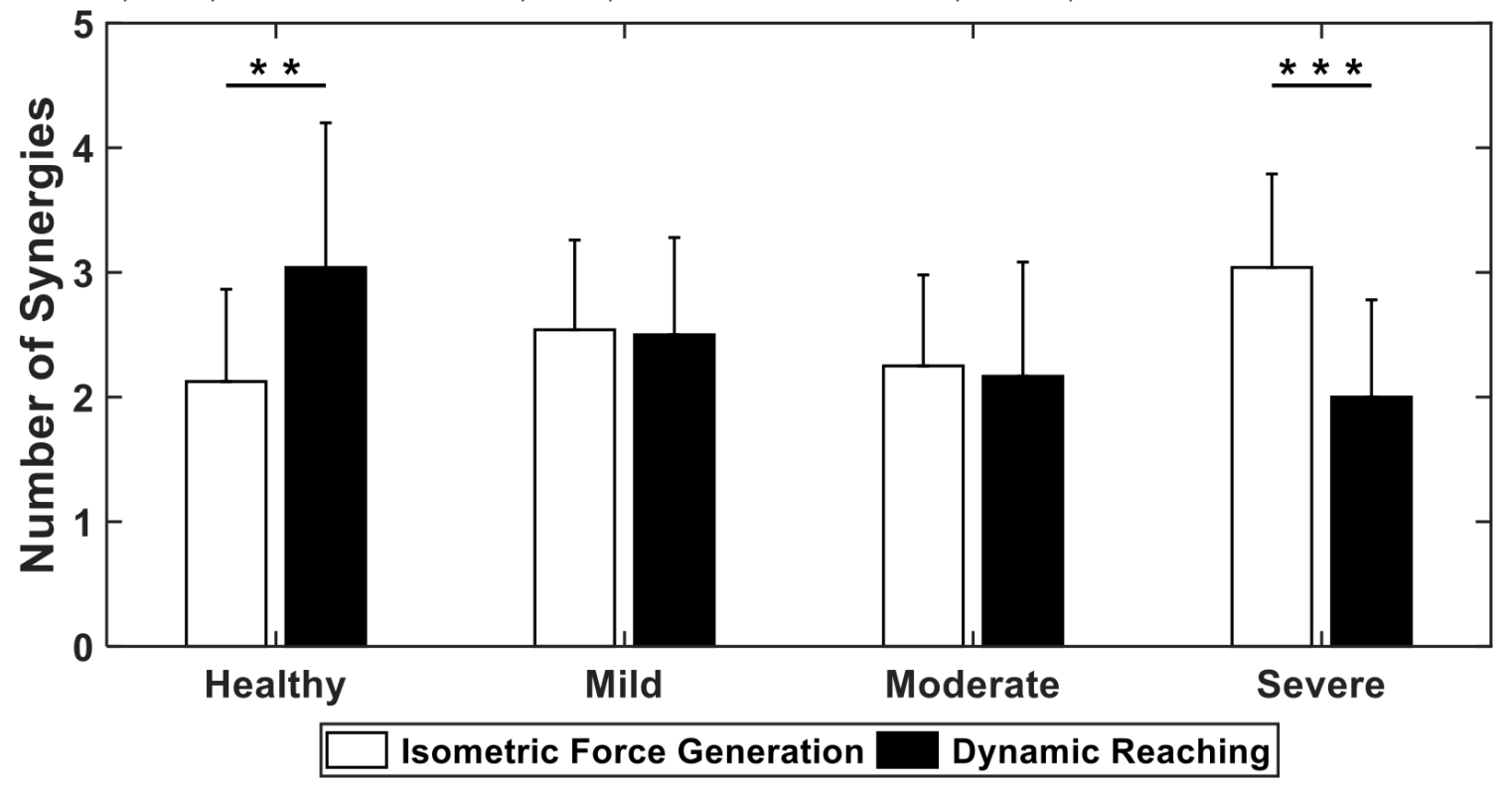
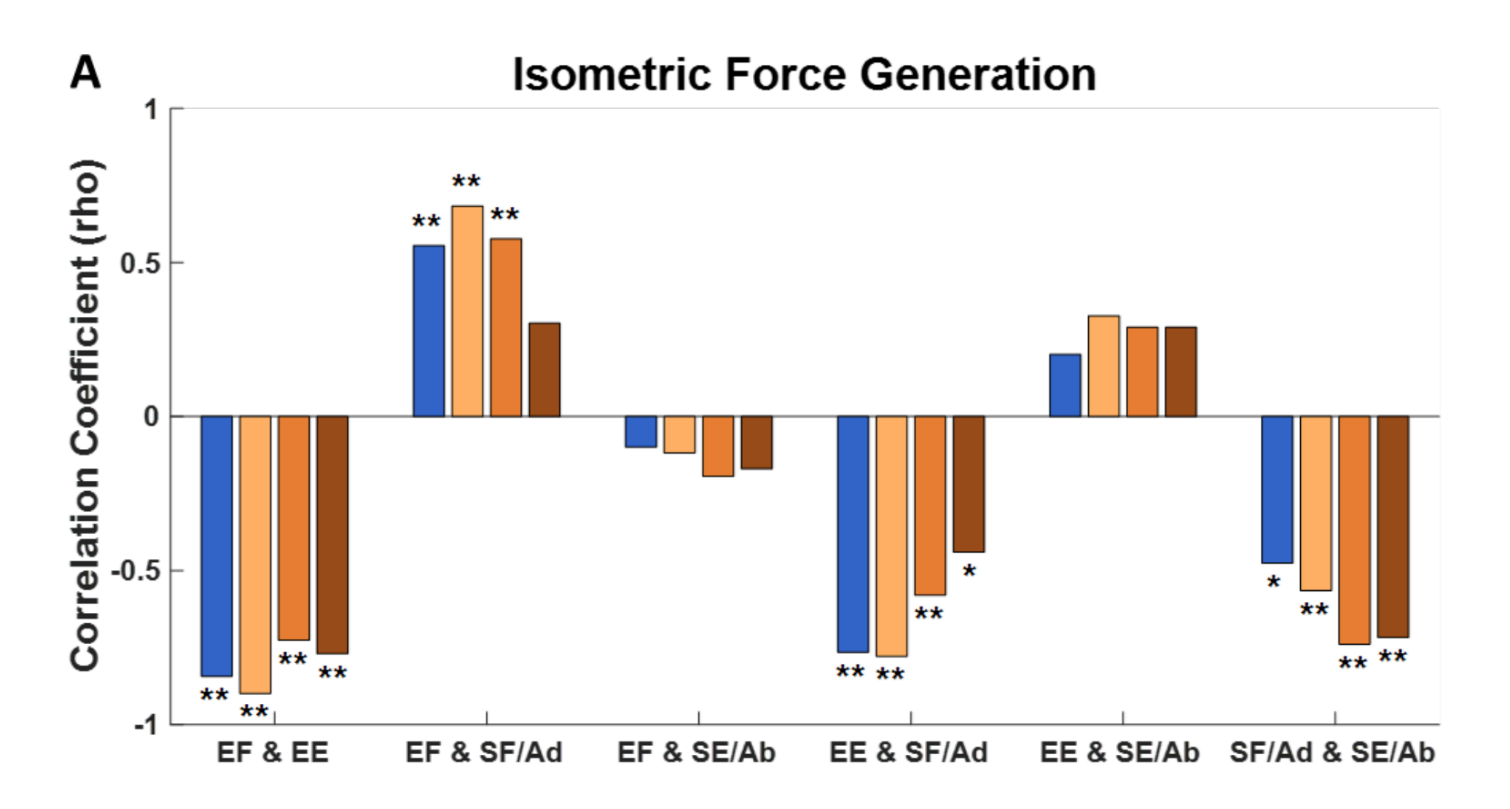


Figure 9

The average number of muscle synergies significantly activated across the 24 targets in both planes for the four subgroups. Wilcoxon signed-rank test showed that healthy participants activated a significantly greater number of synergies across the 24 target directions during the dynamic task than during the isometric task (***, p < 0.01). In contrast, stroke survivors with severe motor impairment activated a greater number of synergies during the isometric task than during the dynamic task (****, p < 0.001). No significant difference was found between the two tasks in the mildly and moderately impaired stroke subgroups.



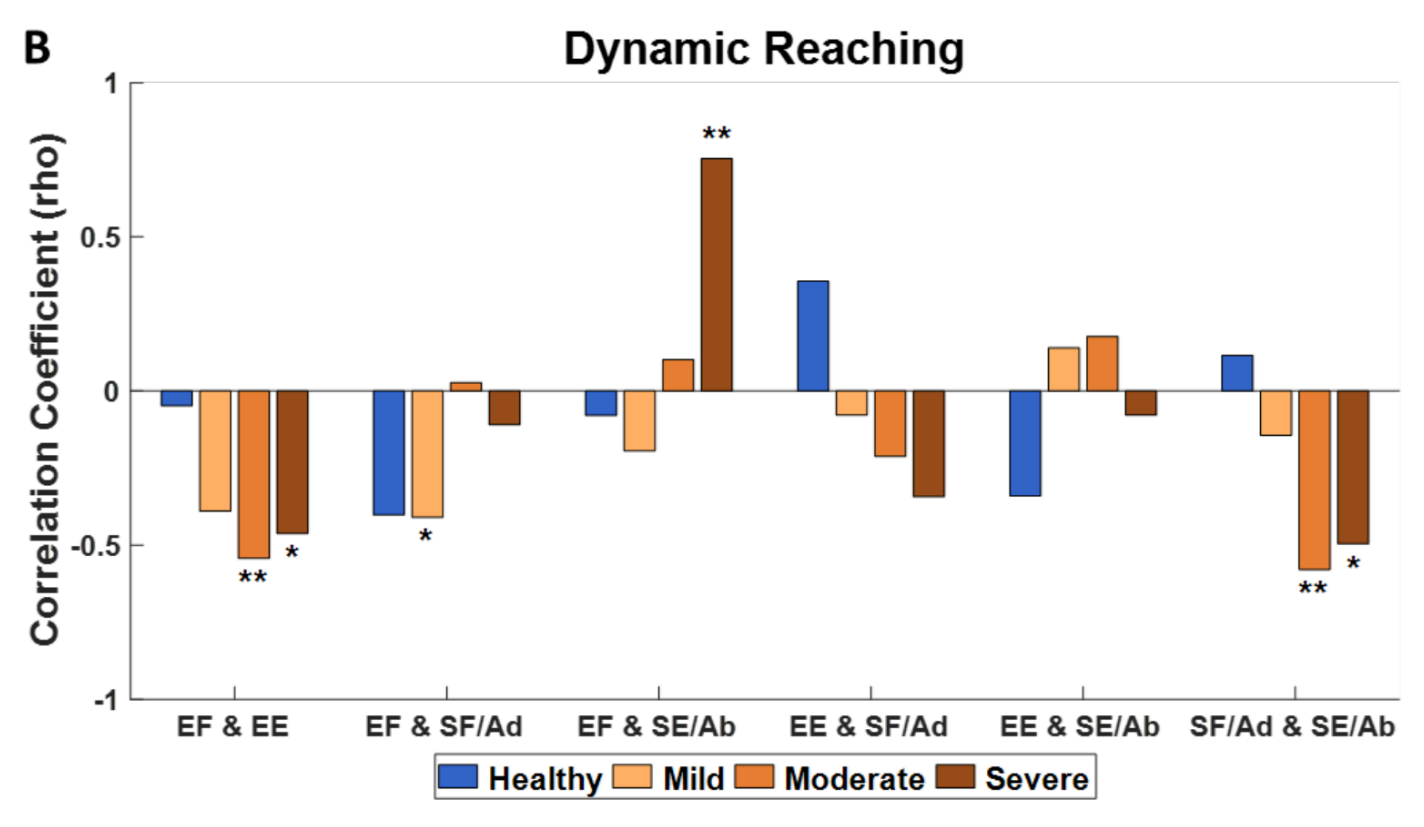


Figure 10

The correlation coefficients of any possible pairs of synergy activation profiles averaged across participants in any subgroup (Spearman correlation, *, p < 0.05; **, p < 0.01) during the isometric force generation task (**A**) and the point-to-point reaching task (**B**). EF, elbow flexor; EE, elbow extensor; SF/Ad, shoulder flexor/adductor; and SE/Ab, shoulder extensor/abductor.

Supplementary Files

This is a list of supplementary	files associated with this	preprint. Click to download.

• Table1.docx